ELSEVIER

Contents lists available at ScienceDirect

Journal of Hydrology

journal homepage: www.elsevier.com/locate/jhydrol



Research papers

The directional unit hydrograph model: Connecting streamflow response to storm dynamics[☆]

Gabriel Perez a,*, Jesus D. Gomez-Velez b,a,*, Xingyuan Chen c, Timothy Scheibe c

- ^a Civil and Environmental Engineering, Vanderbilt University, Nashville, TN, USA
- ^b Environmental Sciences Division & Climate Change Science Institute, Oak Ridge National Laboratory, Oak Ridge, TN, USA
- ^c Pacific Northwest National Laboratory, Richland, WA, USA

ARTICLE INFO

This manuscript was handled by Andras Bardossy, Editor-in-Chief, with the assistance of Sheng Yue. Associate Editor.

Dataset link: https://github.com/gomezvelezlab/Directional-UH

Keywords:
Directional unit hydrograph
Width function
Storm motion
Storm velocity
Peak flow

ABSTRACT

Storm velocity (i.e., direction and speed) and structure (i.e., shape and intensity) play a critical role in streamflow response. These characteristics determine the timing and magnitude of precipitation fluxes across the watershed that drive runoff generation and conveyance along the river network. While previous efforts have used spatially explicit hydrologic models to assess the role of storm properties in streamflow magnitude, their computational demand significantly limits the range of scenarios that can be explored, hindering our ability to systematically identify critical conditions leading to extreme events. To address this technical gap, we introduce the Directional Unit Hydrograph (Directional-UH) model, a parsimonious approach based on the classic theory of the Unit Hydrograph. The Directional-UH extends the original theory by relaxing the assumption of spatial uniform rainfall and incorporating storm direction and speed into the unit hydrograph function. The model conceptualizes storms as rectangular structures with constant intensity moving along a linear trajectory with constant speed. We verify and validate our conceptualization by comparing with simulations, based on observations of extreme rainfall events, of the distributed hydrological model Hillslope-Link-Model (HLM) in the Turkey River basin in Iowa, USA. Then, the Turkey River basin is used as a testbed to illustrate three practical applications of the Directional-UH model. First, we identify the storm trajectory that produces the highest peak flow response. Second, we determine the storm characteristics that maximize the peak flow response by synchronizing storm motion and flood wave; we refer to this as the resonance condition. Third, we systematically explore the compounding effects of consecutive storm events with different trajectories to identify critical combinations that exacerbate the peak flow magnitude. The results on our testbed demonstrate that storm velocity has the potential to increase by a factor of two the peak flow magnitude when compared to stationary storm events. Overall, the parsimonious nature of the Directional-UH model offers a unique and valuable tool for modeling, predicting, and interpreting rainfall-runoff dynamics through the lens of storm direction, speed, and structure.

1. Introduction

Empirical observations and global climate model projections show that the intensity, duration, frequency, and spatial extent of rainfall events are being affected by changes in atmospheric circulation patterns, with a high potential impact on storm trajectories. For example, climate models project a poleward shift of storm tracks at the end of this century (Mbengue and Schneider, 2013; Tamarin-Brodsky and

Kaspi, 2017). Furthermore, analysis of historical rainfall data in the contiguous United States shows that a large proportion of the eastern United States has seen a clockwise trend in the dominant direction of precipitation (Goodwell, 2020). This evidence is significant in flood prediction because laboratory experiments (de Lima and Singh, 2003) and model-driven simulations (Gao and Fang, 2019; Seo and Schmidt, 2013) show that storm trajectories can change drastically and affect the

Notice: This manuscript has been co-authored by staff from UT-Battelle, LLC, under contract DE-AC05-00OR22725 with the US Department of Energy (DOE). The US government retains and the publisher, by accepting the article for publication, acknowledges that the US government retains a nonexclusive, paid-up, irrevocable, worldwide license to publish or reproduce the published form of this manuscript, or allow others to do so, for US government purposes. DOE will provide public access to these results of federally sponsored research in accordance with the DOE Public Access Plan (http://energy.gov/downloads/doe-public-access-plan)

^{*} Correspondence to: Environmental Sciences Division & Climate Change Science Institute, Oak Ridge National Laboratory, Oak Ridge, TN, USA. E-mail addresses: perezmesagj@ornl.gov (G. Perez), gomezvelezjd@ornl.gov (J.D. Gomez-Velez).

magnitude and duration of flood events. As climate change disturbs typical patterns of storm trajectories, catchments are likely to experience new rainfall forcing, leading to unseen extreme responses. A transition that will be reflected in individual events and the statistics of peak flows. Understanding how these potential changes in forcing will affect hydrologic response is critical for designing resilient flood protection infrastructure under future climate scenarios.

Process-based hydrological models serve as a platform to test and validate conceptualizations of hydrological processes and quantify how flood magnitudes will change due to natural and anthropogenic perturbations in the hydrological system. For instance, previous efforts have used distributed hydrological models to evaluate the effect of storm direction on streamflow generation (e.g., Gao and Fang, 2019; Ghimire et al., 2021; Perez et al., 2021), finding significant changes in the mechanisms generating runoff and flood wave propagation. In particular, Perez et al. (2021) used a distributed hydrological model to evaluate how changes in preferential storm trajectory will affect the probability distribution of peak flows, not just individual events. Using a 20,000 km² agricultural basin in the Midwest USA as a testbed and thousands of simulations for individual storms, they show that the 100-year flood can increase up to 25% due to changes in storm direction.

The modeling efforts highlighted above require the implementation, calibration, and validation of distributed hydrological models with many parameters (ranging from tenths to even hundreds), significant computational resources, and a high level of modeling expertise. These modeling requirements limit the ability of researchers to explore a broad range of scenarios and preclude widespread application by practitioners. To overcome this challenge, parsimonious hydrological models have been used as an alternative to complex distributed hydrological models. Parsimonious hydrological models focus on critical processes and only require a few model parameters. Given their simplicity, these models have been widely adopted by researchers and practitioners to assess hydrological systems by focusing on model structures that are transferable and reproducible. For example, the Unit Hydrograph (UH) (Sherman, 1932) model is one of the most common parsimonious conceptualizations for rainfall-runoff transformation. The UH is a clear example of how a simple, elegant, and robust model formulation can permeate to practitioners to become a fundamental tool for predicting peak flow magnitudes in engineering design (Singh et al., 2014; Bhunya, 2011).

In the spirit of these parsimonious modeling approaches, the main objective of this work is to present a transferable and reproducible hydrological model for streamflow that explicitly represents storm velocity (direction and speed) and structure (shape and intensity): the *Directional Unit Hydrograph* (Directional-UH). In simple terms and from a conceptual perspective, the Directional-UH computes hydrographs by simplifying observed storm structures into equivalent rectangular moving storms (see Fig. 1). The following sections show that the Directional-UH extends the UH approach while maintaining conceptual simplicity and computational efficiency.

After formulating the Directional-UH model, we use a higher-complexity hydrologic model to verify and validate its predictions in a testbed watershed. Then, we illustrate the Directional-UH potential by addressing three fundamental questions. First, what storm direction and speed maximize the peak flow response? Second, what physical conditions are required to trigger a resonance effect between the storm motion and the flood wave propagation that maximizes the peak flow response? And third, given two consecutive storm events, what is the combination of storm trajectories that maximizes the peak flow response? The modest computational demand of the Directional-UH makes it particularly well suited to answer these questions given the need to explore many combinations of storm structure and velocity and initial hydrological conditions (e.g., antecedent soil moisture, initial streamflow), which are evolving in space and time (Singh et al., 2014; Perez et al., 2019a).

2. The foundation: The Unit Hydrograph

If a watershed behaves linearly, the Unit Hydrograph (UH) represents the direct runoff response at its outlet resulting from a unit volume of effective rainfall applied uniformly throughout the entire domain at a constant rate over a specific duration (Sherman, 1932). It is further assumed that the UH is time-invariant and does not change with the characteristics of rainfall or watershed properties. In the limit, for an infinitesimally small rainfall duration, we refer to the UH as the Instantaneous Unit Hydrograph (IUH), which describes the hydrologic response to a unit volume of effective rainfall applied instantaneously throughout the watershed. Again, assuming that the watershed behaves as a linear system, the outlet's streamflow response (Q(t); $[L^3T^{-1}]$) at any time t is estimated as the convolution of the input function rate ($J_e(t)$; $[LT^{-1}]$) and the IUH (g(t); $[T^{-1}]$) (Dooge, 1973):

$$Q(t) = A \int_0^t J_e(\tau)g(t-\tau) d\tau, \tag{1}$$

where $A[L^2]$ is the watershed drainage area and $J_e(t)$ represents the effective rainfall intensity that is assumed to occur spatially uniform throughout the watershed. The effective rainfall, $J_o(t)$, is defined by rainfall characteristics (intensity and duration), soil properties, and antecedent soil moisture conditions. The IUH function, g(t), which is also commonly referred to as the transfer function or the kernel function, encapsulates the runoff generation mechanisms within the watershed. Several strategies have been proposed to estimate it (Bernard, 1935; Snyder, 1938; Taylor and Schwarz, 1952; Murphey et al., 1977; Rodríguez-Iturbe and Valdés, 1979; Croley, 1980; Gupta et al., 1980; Aron and White, 1982; Singh, 1964; Bras and Rodriguez-Iturbe, 1989; Yen and Lee, 1997; Bhunya et al., 2009; Patel and Thorvat, 2016; Guo and Asce, 2022; Guo, 2022; Huang and Lee, 2023; Yi et al., 2022), and among those approaches, the ones that link the watershed's measurable geomorphological and hydraulic characteristics have become particularly popular (Snell and Sivapalan, 1994; Rigon et al., 2016). For example, the Geomorphological Instantaneous Unit Hydrograph (GIUH), first proposed within a probabilistic framework by Rodríguez-Iturbe and Valdés (1979), generalized by Gupta et al. (1980) and formalized by Rinaldo and Rodruiguez-Iturbe (1996), connects g(t)with the watershed's morphology and channel hydraulics using the Horton-Strahler ordering technique, offering simple predictive expressions for the magnitude and timing of peak flows. In the same vein, the Width Function Instantaneous Unit Hydrograph (WFIUH) (Kirkby, 1976) relaxes the assumption of a theoretical probability distribution for g(t) and instead uses an estimated travel time distribution based on isochrones calculated from drainage paths derived from digital elevation models. This empirical representation better captures the physical processes that dominate runoff generation and streamflow channel routing with widely available data. These isochrones, under some hydrodynamic assumptions, can be derived from the width function $(W(x); [L^{-1}])$ of the watershed. The W(x) denotes the number of sites at the distance x [L] to the outlet of the watershed, where the distance x is calculated along the surface flow path. In general, it is convenient to represent W(x) as a probability distribution, and therefore, W(x)is normalized so that its integral equals unity. The width function has been used in different studies as a fundamental morphological descriptor of watershed hydrology with particular controls on runoff generation and peak flow response (Moussa, 2008a,b; Perez et al., 2019a, 2018).

Within the WFIUH framework, we can distinguish between travel times in channels and hillslopes by replacing W(x) with the rescaled width function, $W_{c,h}(x)$ [L⁻¹], which is obtained by rescaling distance as

$$x'_{c,h} = x_c + \frac{u_c}{u_b} x_h, (2)$$

where u_h [LT⁻¹] is the hillslope flow celerity, u_c [LT⁻¹] is the channel flow celerity, x_h [L] is the hillslope distance along the surface drainage

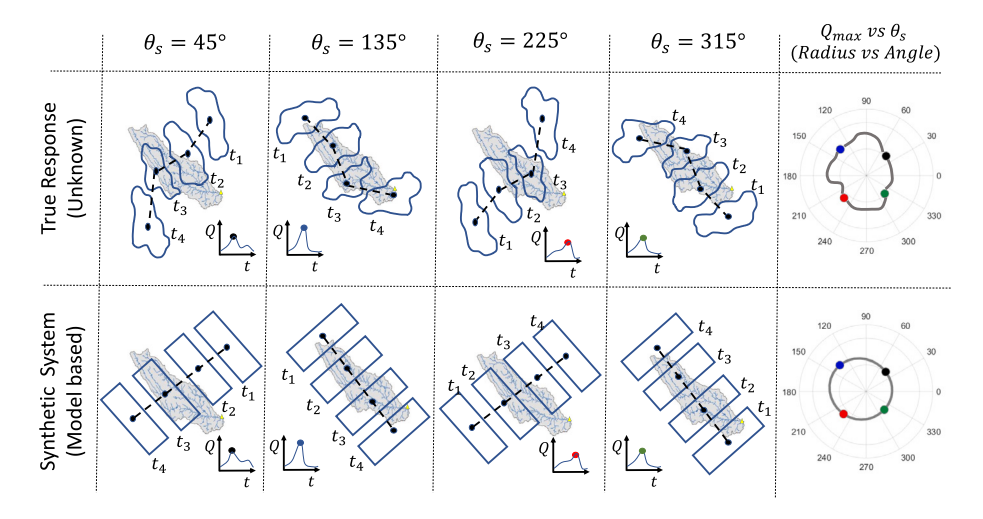


Fig. 1. Illustration of the transformation from observed storms (top panels) to rectangular moving storms (bottom panels) for different storm trajectories. The direction of the storm trajectory is represented by θ_s . The circular plots in the right panels illustrate the peak flows, Q_{max} (radius), at the outlet of the watershed as a function of the storm direction, θ_s (angle).

path to the closest channel, and x_c [L] is the channel distance to the outlet of the watershed (Rinaldo et al., 1995). Because the hillslope flow celerity is significantly lower than the channel celerity, this rescaled width function significantly improves the physical representation and predictability of the WFIUH (Botter and Rinaldo, 2003; Grimaldi et al., 2010, 2012; Di Lazzaro and Volpi, 2011). Fig. 2C-D highlights the differences between W(x) (panel C) and $W_{c,h}(x)$ (panel D) for our testbed watershed. In this case, $W_{c,h}(x)$ is smoother due to the effect of longer travel times for water particles starting their journey on hillslopes.

For the WFIUH model, g(t) is estimated as

$$g(t) = \int_0^{L_{max}} W_{c,h}(x) f(t|x) dx$$
(3)

where f(t|x) [T⁻¹] is the travel time distribution for a path of length x and L_{max} [L] is the longest drainage path under the rescaled distance $x'_{c,h}$. When the effects of hydrodynamic dispersion are negligible, the water is subject mainly to advection (kinematic wave), and the probability distribution of the travel time for a rainwater particle falling at a distance x from the outlet is

$$f(t|x) = u_c \,\delta\bigg(t - \frac{x}{u_c}\bigg) \tag{4}$$

with $\delta(\cdot)$ the Dirac delta function. Substituting Eq. (3) into Eq. (4) provides an expression for the IUH:

$$g(t) = u_c W_{c,h}(u_c t). \tag{5}$$

At a higher level of complexity, the formulation of f(t|x) can include the effects of flow response smoothing caused by hydrodynamic dispersion (Mesa and Mifflin, 1986; Rinaldo et al., 1991; van de Nes, 1973):

$$f(t|x) = \frac{x}{\sqrt{4\pi Dt^3}} \exp\left[-\frac{(x - u_c t)^2}{4Dt}\right]$$
 (6)

where D [L²T⁻¹] is the hydrodynamic dispersion coefficient. In this case, the IUH is given by

$$g(t) = \int_0^{L_{max}} \frac{x W_{c,h}(x)}{\sqrt{4\pi D t^3}} \exp\left[-\frac{(x - u_c t)^2}{4Dt}\right] dx.$$
 (7)

The kinematic case can be obtained from Eq. (7) when $D \to 0$. Finally, the streamflow at the watershed outlet using the kinematic and hydrodynamic dispersion approach is given by

$$Q(t) = A \int_0^t J_e(\tau) u_c W_{c,h}(u_c(t-\tau)) d\tau$$
(8)

and

$$Q(t) = A \int_0^t J_e(\tau) \int_0^{L_{max}} \frac{x W_{c,h}(x)}{\sqrt{4\pi D(t-\tau)^3}} \exp \left[-\frac{(x-u_c(t-\tau))^2}{4D(t-\tau)} \right] \mathrm{d}x \, \mathrm{d}\tau. \tag{9}$$

Here, it is important to highlight two crucial assumptions implicit in Eqs. (8) and (9). First, the parameters u_c , u_h , and D are assumed constant for the watershed. However, in natural systems, flow celerities and dispersion vary in space and time with channel geometry, surface roughness, and flow magnitude (Beven, 2020); therefore, these parameters would be considered effective for the system. Second, rainfall is assumed uniform, which misrepresents the spatial–temporal dynamics of observed rainfall fields. These assumptions allow for a parsimonious model but can hinder the ability of the UH to describe and predict hydrologic response for storms evolving in space and time.

To relax the latter assumption, previous studies incorporated the effects of spatially distributed rainfall into the UH (Naden et al., 1999; Smith et al., 2005; Emmanuel et al., 2015). In general, this is done replacing $W_{c,h}(x)$ by the rainfall width function, $W_R(x,t)$ [L⁻¹], defined

$$W_{R}(x,t) = \frac{\bar{J}_{e}(x,t)}{\bar{J}_{o}(t)} W_{c,h}(x)$$
 (10)

where $\bar{J}_e(x,t)$ [LT⁻¹] is the average effective rainfall intensity at time t falling at a location with a surface flow path distance x from the watershed outlet, and $\bar{J}_e(t)$ [LT⁻¹] is the mean value of the effective rainfall intensity within the watershed at time t.

Unlike $W_{c,h}(x)$, the rainfall width function $W_R(x,t)$ is time-dependent and must be recalculated for every rainfall event, making its use difficult in practice. To overcome this obstacle, Andrieu et al. (2021) proposed the Event-WFIUH by assuming that the spatial and temporal effects of effective rainfall can be isolated as

$$\bar{J}_e(x,t) = W_e(x)\bar{J}_e(t) \tag{11}$$

where $W_e(x)$ [L⁻¹] is the event width function. This function is time-independent and estimated from inverse techniques by finding the best representation of $W_e(x)$ that reconstructs the observed hydrograph for a specific rainfall-runoff event. In particular, since that $W_e(x)$ is estimated from inverse techniques using streamflow observations, $W_e(x)$ is suitable for the characterization of rainfall-runoff signatures for a given observed flood event but not specifically useful for analyzing and predicting the effects of storm dynamics on streamflow response.

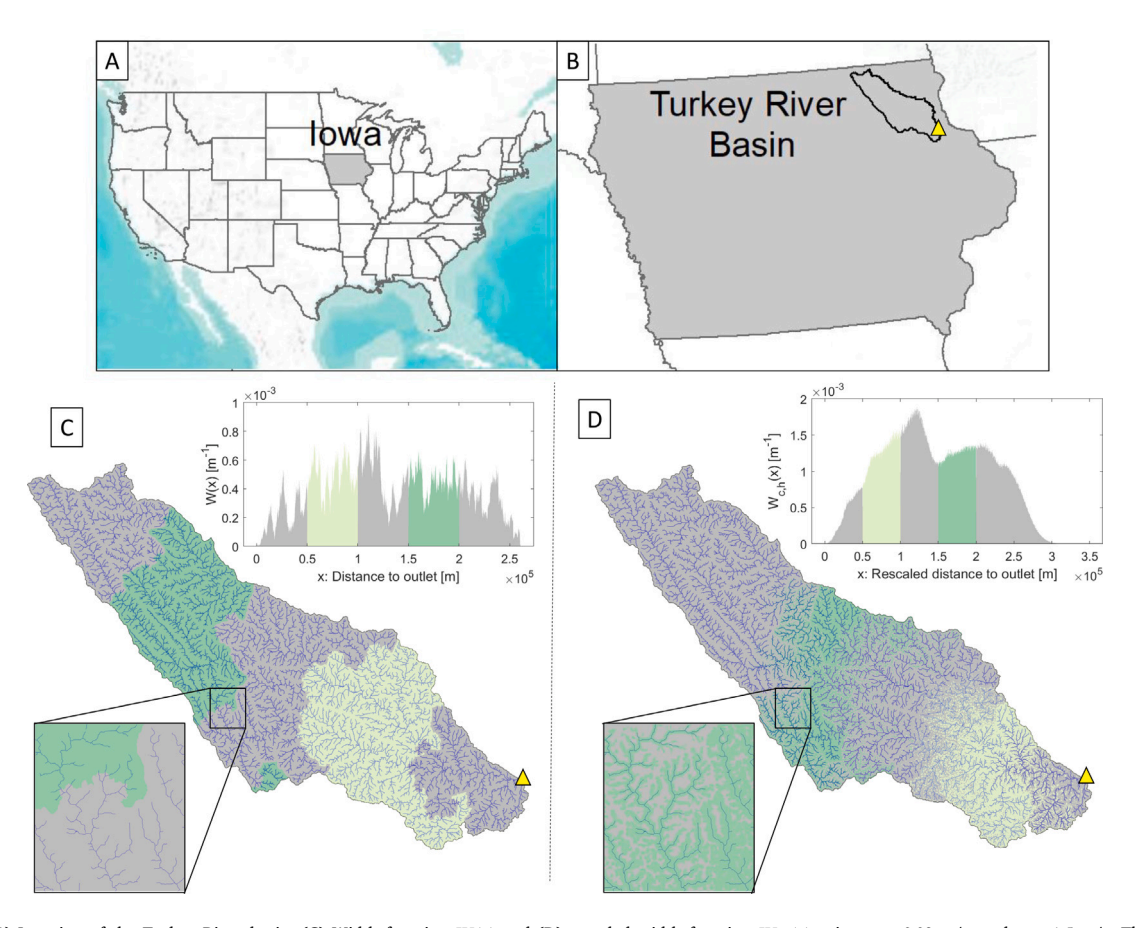


Fig. 2. (A and B) Location of the Turkey River basin. (C) Width function W(x) and (D) rescaled width function $W_{c,h}(x)$ using $u_h = 0.02$ m/s, and $u_c = 1.5$ m/s. The strip areas in panels C and D are associated with a specific distance to the basin outlet. The yellow triangle shows the location of the watershed outlet.

3. The Directional Unit Hydrograph

As the previous section shows, the WFIUH model has evolved significantly from its original formulation to represent spatially distributed rainfall and differentiate between travel times in hillslopes and channels. However, the WFIUH's current formulation still ignores critical storm characteristics such as velocity (i.e., direction and speed) and structure (i.e., shape), hindering its ability to capture the complex spatiotemporal dynamics of hydrologic response. With this in mind, we present a new formulation of the WFIUH: the Directional Unit Hydrograph (Directional-UH).

First, we discretize the landscape into hydrologic response units (HRUs) where the parameters and states are assumed spatially uniform. For simplicity, we use squared elements of length Δx to represent HRU, and the centroid of a given HRU j is denoted by the coordinates (x_j, y_j) . Second, we parameterize storm motion and structure characteristics. In this case, we use the following assumptions to simplify the storm dynamics (Fig. 3A):

- The storm is generated outside the modeling domain and traverses the watershed without changing shape.
- 2. The storm has constant intensity i_s [L] and rectangular area with length I_s (storm front length, [L]) and width w_s (lateral storm length, [L]). Moreover, the rectangular storm front, I_s , is larger than the diameter of the circumscribed circle of the watershed boundary.
- 3. The rectangular storm moves along a linear trajectory perpendicular to the storm front with constant speed v_s [LT⁻¹] and direction θ_s . The angle θ_s is measured in a counterclockwise direction from the line defined by points (x_b, y_b) and (∞, y_b) to the line defined by points $(x_{s,0}, y_{s,0})$ and (x_b, y_b) . Here, the point

 (x_b, y_b) is the watershed centroid, and the point $(x_{s,0}, y_{s,0})$ is the center point of the storm front at the beginning of the event.

The assumptions above provide a significant degree of flexibility to represent storm dynamics while maintaining the mathematics tractable and the implementation numerically inexpensive. The are two main benefits of conceptualizing the storm structure as a rectangular moving storm with constant velocity. First, the travel time for the storm front to reach any HRU can be easily calculated. More specifically, the distance from the initial location of the storm front line to any HRU j, x_s , is given by the perpendicular euclidean distance between the HRU's centroid (x_i, y_i) and the storm front line at the initial location $(x_{s,0}, y_{s,0})$ (see Fig. 3A). Then, given that the storm moves with constant speed v_s , the time required for the storm front to reach the HRU *j* is calculated as x_{s_i}/v_s . Second, although each HRU receives rainfall at different times, the time of rainfall duration $(D_s = w_s/v_s; [T])$ is the same for all HRUs, and therefore, all HRUs receive the same rainfall volume (and intensity). Here, D_s represents the period of time during which an HRU receives rain from the rectangular storm event, and it should not be confused with the time it takes for the rectangular storm to cross the entire watershed. In summary, the hietogram for any HRU j can be easily predicted as a function of x_s , v_s , θ_s , D_s , and i_s .

We incorporate the storm dynamics for this rectangular storm into the WFIUH model by adding the travel time of the storm front to each HRU, which propagates into the watershed's width function. To this end, the distance x_s is incorporated as a rescaled distance in the width function estimation. Then, similar to the distinction of travel times between hillslopes and channels, the Directional-UH is constructed by accounting for the arrival time of the rectangular storm event to each HRU within the watershed with a rescaled distance

$$x'_{c,h,s} = x_c + \frac{u_c}{u_h} x_h + \frac{u_c}{v_s} x_s.$$
 (12)

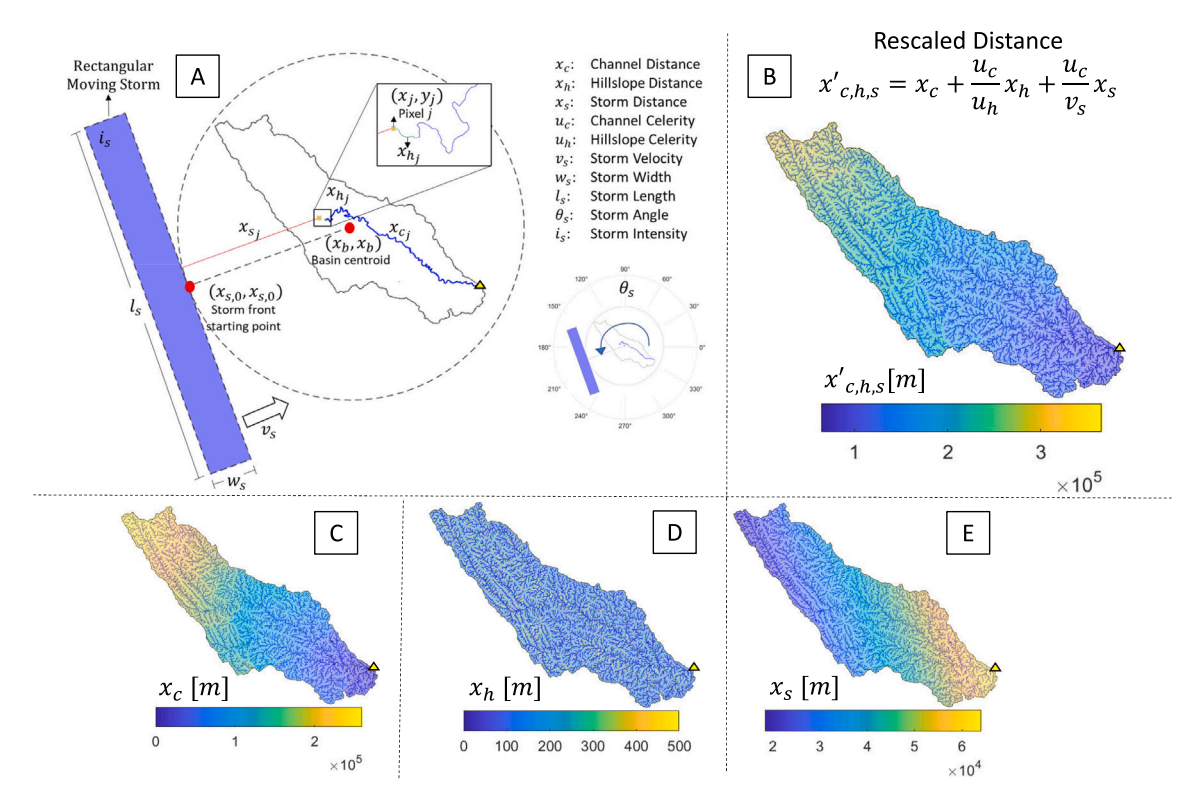


Fig. 3. (A) Key components characterizing the rectangular moving storm used in the Directional-UH. (B) Rescaled distances accounting for storm distance and hillslope distance. Maps with (C) the channel distance, x_c , (D) the hillslope distance, x_h , and (E) the storm distance, x_s .

and its corresponding rescaled width function, $W_{c,h,s}(x)$ [L⁻¹]. Here, it is important to highlight two important aspects of the rescaled distance definition in Eq. (12). First, note that the distance x_s depends on the initial location of the storm front $(x_{s,0},y_{s,0})$ and the storm direction, θ_s , as a result the distance $x'_{c,h,s}$ also depends on the storm properties v_s and θ_s . Second, Eq. (12) uses the storm speed v_s and not celerity, because celerity is only considered in the domain where the flood wave travels, which in this case occurs only over hillslopes (u_b) and channels (u_c) .

The IUH resulting from replacing W(x) in Eq. (3) by $W_{c,h,s}(x)$ is termed as the Instantaneous Directional Unit Hydrograph (IDUH). Formally, the IDUH represents the streamflow response due to an instantaneous unitary rainfall intensity pulse from a rectangular storm moving with constant speed, v_s , along a linear trajectory described by the storm direction, θ_s . The IDUH already incorporates the travel time for the storm front to reach every HRU. Furthermore, because each HRU receives the same rainfall intensity i_s during time D_s , the effective rainfall. $I_s(t)$, is defined as

$$J_e(t) = \begin{cases} RC \cdot i_s & \text{for } t_0 < t \le t_0 + D_s \\ 0 & \text{otherwise} \end{cases}$$
 (13)

where t_0 is the storm starting time at the initial storm front point $(x_{s,0}, y_{s,0})$ and RC is the spatially uniform runoff coefficient representing the proportion of rainfall becoming runoff. Then, replacing the new rescaled width function and the effective rainfall into Eqs. (8) and (9), we obtain the Directional-UH model for the kinematic and hydrodynamic dispersion cases with uniform runoff coefficient:

$$Q(t) = A \int_0^t J_e(\tau) u_c W_{c,h,s}(u_c(t-\tau)) d\tau$$
 (14)

$$Q(t) = A \int_0^t J_e(\tau) \int_0^{L_{max}} \frac{x W_{c,h,s}(x)}{\sqrt{4\pi D(t-\tau)^3}} \exp\left[-\frac{(x-u_c(t-\tau))^2}{4D(t-\tau)}\right] dx d\tau$$
(15)

where in this case L_{max} is the longest rescaled distance $x'_{c,h,s}$.

In this model, $J_e(t)$ is a function of i_s and D_s , and $W_{c,h,s}(x)$ is a function of the landscape, river network and the storm parameters v_s and θ_s . The latter relationship is illustrated in Fig. 4, where $W_{c,h,s}(x)$ was estimated for different values of θ_s with a v_s of 3 m/s. The changes in the rescaled width function highlight the significant differences for storm trajectories traveling downstream (Fig. 4B) versus those traveling upstream (Fig. 4D). These changes in $W_{c,h,s}(x)$ will be reflected in significantly different peak flow magnitudes (see Section 5.3.1).

Finally, we propose three variations of the Directional-UH model formulation to represent a broader range of hydrological scenarios. First, spatially variable runoff coefficients can be incorporated by superposing the streamflow response from individual IDUHs calculated for HRUs associated with a specific class of runoff coefficient. Mathematically, this can be expressed as

$$Q(t) = \sum_{k=1}^{N_{RC}} A_k \int_0^t J_{e_k}(\tau) g_k(t - \tau) d\tau$$
 (16)

$$J_{e_k}(t) = \begin{cases} RC_k \cdot i_s & \text{for } t_0 < t \le t_0 + D_s \\ 0 & \text{otherwise} \end{cases}$$
 (17)

where N_{RC} [-] is the number of runoff coefficient classes, A_k [L²] is the drainage area of the HRUs within RC class k, $g_k(t)$ [T⁻¹] is the IDUH calculated from the HRUs within runoff coefficient class k, $J_{e_k}(t)$ [LT⁻¹] is the effective rainfall for runoff coefficient class k, and RC_k is the runoff coefficient for class k.

A second model variation is to incorporate temporal changes in rainfall intensity. This can be done by replacing the constant rainfall intensity i_s with a hyetograph $i_s(t)$ representative of the temporal variation of rainfall at the initial storm location $(x_{s,0}, y_{s,0})$. In this case, each HRU will observe the same hyetograph but shifted by a time $x_{s,j}/v_s$. A third variation is to use storm fronts, l_s , smaller than the diameter of the circumscribed circle of the watershed boundary. This is of particular interest for modeling storm events partially covering the watershed, which is commonly expected in large river basins. To achieve the effect of partial storm coverage in the Directional-UH,

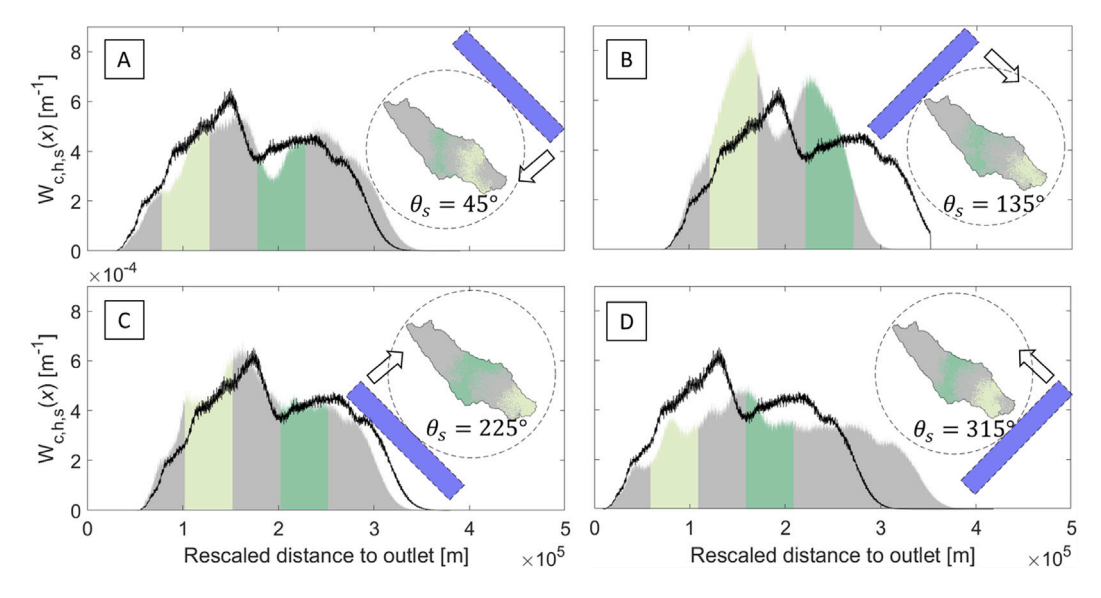


Fig. 4. Examples of the rescaled width function, $W_{c,h,s}$, for storm angles of $\theta_s = 45^\circ$ (A), $\theta_s = 135^\circ$ (B), $\theta_s = 225^\circ$ (C), and $\theta_s = 315^\circ$ (D). The rescaled distances were calculated using $v_s = 3$ m/s, $u_c = 1.5$ m/s, and $u_h = 0.02$ m/s. The black lines represent the rescaled width function, $W_{c,h}$, which does not consider the storm directions. Note that for comparison purposes, the rescaled width function, $W_{c,h}$, was translated to the first value of $W_{c,h,s}$ that is different from zero.

the width function $W_{c,h,s}(x)$ must be calculated from only the HRUs receiving rain, and the drainage area, A, must reflect only the sum of the area that encompasses these HRU locations. The general approach to implement the Directional-UH model includes the following steps. (i) Estimate the width function at the relevant basin outlet. (ii) Calibrate and validate the model parameters using observed data (details in section 4.3). (iii) Set parameter ranges representing storm dynamics (i.e., extent, intensity, duration, and velocity) based on realistic storm structures. (iv) Use the Directional-UH model (Eqs. (14) or (15)) to systematically explore the dynamics of streamflow response as a function of the storm's characteristics.

4. Case study and methods

We use the Turkey River watershed (Fig. 2A–B) in Iowa, USA, as a testbed to assess the strengths and limitations of the Directional-UH model for the case of constant runoff coefficients. This agricultural watershed, with a drainage area of $4385 \, \mathrm{km^2}$, has been extensively studied in the context of changes in peak flow dynamics resulting from spatial and temporal patterns of storms (Zhu et al., 2018), seasonal changes in snowmelt and soil moisture (Yu et al., 2019), global climate projections (Yu et al., 2020), and, in particular, changes in storm direction (Perez et al., 2021). All these previous studies make this watershed an ideal candidate for expanding the understanding of physical controls on flood generation, specifically in terms of storm structure and velocity (direction and speed).

To implement the Directional-UH model within the Turkey River watershed, we define HRUs and their hydrological connectivity (flow direction) using a 30-m digital elevation model (DEM) from the National Hydrography Dataset (NHDPlus Version 2.1 accessed on Jun 1, 2021.). This definition implicitly assumes that a spatial resolution of 30 m can capture the spatial–temporal evolution of rainfall fields. Also, we use Stage-IV radar rainfall data (Du, 2011) (more details in Section 4.1) to parameterize the rectangular moving storms needed for the Directional-UH implementation.

In the following subsections, we describe the four components of our approach to assessing the assumptions and performance of the Directional-UH model. The first component focus on estimating equivalent parameters to define rectangular moving storms from observed radar rainfall fields. The second component uses the distributed hydrological model Hillslope-Link-Model (HLM) to estimate and compare the hydrographs resulting from the observed storms and their equivalent

rectangular representations defined by the first component. The third component focuses on the calibration and validation of the Directional-UH model. Lastly, the fourth component uses the Directional-UH to explore the watershed response dynamics, emphasizing critical trajectories and compounding storms that exacerbate peak flow magnitude.

4.1. Estimation of equivalent rectangular storm parameters

This section describes the procedure to select storm events from observations and the processes to transform such events into equivalent rectangular storms (i.e., going from the top row to the bottom row in Fig. 1). This is a critical step to verify if actual storm events can be represented with rectangular moving storms and how these assumptions impact our estimates of the hydrologic response. This component is subdivided into two steps: (i) identify the storm events that could occur within the Turkey River watershed and (ii) characterize the storm properties by tracking the migration of the identified storms.

We use the RainyDay software (Wright et al., 2017) to identify the storm events from the Stage-IV radar rainfall dataset with an approximate spatial resolution of 4km by 4km, and a temporal resolution of one hour from 2002 to 2020 (Du, 2011). A detailed description of the procedure for storm selection with RainyDay from gridded rainfall datasets can be found in Wright et al. (2017). Here, we synthesize the procedure into four main steps. First, the user must define a spatial boundary domain to search for storm events. In our case, we used a domain that covers the entire state of Iowa (latitudes 40.2°N-45°N and longitudes 90.2°W-96.7°W); therefore we can select storm events that are outside the Turkey River watershed (see Fig. 3B). The selection of storm events outside the watershed is reasonable in this case because Iowa's state can be considered a meteorologically homogeneous region (Wright et al., 2017) where similar storm events can occur anywhere within the region. Second, the user must define a time threshold to calculate the accumulated precipitation within the watershed; we used 72 h, which is close to the mean hydrologic response time of the Turkey River watershed. Third, the user must define a boundary where rainfall is accumulated. We used the watershed boundary polygon. Fourth, and focusing on extreme storm events, RainyDay searches within the analysis domain (Step 1) for independent storm events with the highest accumulated precipitation during the prescribed time threshold (Step 2) and over the spatial extension defined by the polygon (Step 3). Using these steps, we identified 350 storm events. It should be noted that previous studies used these same storm events to evaluate flood frequency estimates at the outlet of the Turkey River basin Wright et al. (2017), Yu et al. (2019) and Perez et al. (2019b).

Once the rainfall events are identified, we used the storm identification, tracking, analysis, and nowcasting (TITAN) storm characterization algorithm (Dixon and Wiener, 1993) and the object-based storm identification algorithm proposed by Davis et al. (2006) to characterize the storm properties (e.g., extent, velocity, intensity, duration, and trajectory) for each event. We emphasize that storm cells that move across the watershed have individual velocities, with complex development cycles and dissipation over space and time (Singh, 1997). Because we are describing the overall spatial structure of the storm event and not individual storm cells, our storm characteristics must be seen as descriptors representing the average spatial-temporal evolution of the storm event. Using the properties of each storm event, we estimate the equivalent parameters to represent rectangular moving storms that closely resemble the average properties of the observed storm characteristics. In other words, we define rectangular moving storms that, on average, have the same storm extent, intensity, duration, speed, and direction as those observed by the storm events detected with Rainy-Day. The Appendix section presents additional details for transforming observed storms into rectangular moving storms.

4.2. Verification of the rectangular storm assumption

We adopted a model-driven approach to assessing whether equivalent rectangular storms can be used to represent rainfall-runoff dynamics from observed storms. In this case, we used a distributed hydrological model to estimate the hydrographs resulting from the observed storms and their equivalent rectangular representation. Then, the appropriateness of the rectangular assumption is assessed by a pairwise comparison of the modeled hydrograph.

We used the distributed hydrological model Hillslope-Link-Model (HLM) to estimate the hydrologic response to the 350 storm events detected with RainyDay. The Iowa Flood Center (IFC) developed this model, which has been validated for the state of Iowa (Quintero et al., 2019). Even though different surface and subsurface conceptualizations and channel routing approaches can be incorporated into HLM. The HLM version that the IFC uses for operational purposes in flood prediction incorporates a non-linear channel routing and includes evaporation, infiltration, water ponding on the surface of the hillslope, the effective depth of water in the upper soil layer, and the effective depth of water in the subsurface of the hillslope (Quintero et al., 2019). We use the HLM model version that uses spatially uniform runoff coefficient. By doing this, we remove the effect of the spatial distribution of infiltration processes in the reference hydrographs, effectively making overland flow the dominant process for flood generation. Although it is not conducted in this study, the simplification of the constant runoff coefficient can be relaxed by using HLM versions that include a more realistic representation of infiltration processes, such as the one presented by Jadidoleslam et al. (2022), which incorporates Richard's equation into the HLM formulation. A detailed description of the constant runoff HLM model can be found in Velasquez et al. (2022). Finally, because not all of these storms occur within the Turkey River watershed domain, we spatially transposed each storm to ensure that the main storm core crosses the centroid of the watershed.

4.3. Calibration and validation of the Directional-UH model

To calibrate and validate the Directional-UH model, we use rainfall-runoff simulations from a hydrological distributed model with a higher-fidelity process-based representation of runoff generation mechanisms and channel routing. We refer to these simulations as the *reference simulations*. The HLM model with constant runoff coefficient, briefly described above, is used in this case — more details about this implementation can be found in Velasquez et al. (2022). Once the reference simulations are obtained, they are used to calibrate the Directional-UH

parameters u_c , u_h , and D. These parameters are storm dependent and must be calibrated for each event.

Previous HLM modeling efforts in the Turkey River watershed allow us to reduce the dimensionality of this inverse problem. Quintero et al. (2019) and Ghimire et al. (2022) have shown that a hillslope celerity of $0.02\,\mathrm{m/s}$ is representative of hillslope overland flow and can reasonably capture peak flow response . With this in mind, we assume a $u_h=0.02\,\mathrm{m/s}$, reducing the number of unknown parameters to two (u_c and D). Similar approaches to reduce the number of parameters have been used by other authors. For example, Grimaldi et al. (2012) proposed an empirical relationship between u_h and local landscape slope. Here we use the following procedure to calibrate u_c and D:

- 1. Create a catalog of synthetic stationary storm events. In this case, we create 35 storm events by combining spatially uniform storm intensities $i_s \in [0.25, 0.5, 0.75, 1, 2]$ mm/h and storm durations $D_s \in [1, 3, 6, 12, 24, 48, 72]$ h.
- Create reference simulations. We create the reference simulations by forcing the HLM model with the storm catalog from Step 1. A uniform runoff coefficient of one is used for all simulations. Therefore, the storm intensities defined in Step 1 are also effective storm intensities.
- 3. Estimate the parameters u_c and D for each rainfall-runoff event. In this case, we use the Nelder–Mead simplex algorithm (Lagarias et al., 1998, as implemented in MATLAB) to estimate the values of u_c and D that minimize the sum of the squared root difference between the reference hydrograph obtained in Step 2 and the Directional-UH hydrograph predictions.

As we mentioned before, the model parameters u_c and D must be estimated for each storm event, which is inconvenient for streamflow prediction when a reference hydrograph is unavailable and the model cannot be calibrated. To address this issue, we propose surrogate models (i.e., a fitted function) that relates u_c and D to the rainfall properties i_s and D_s . These models are fitted with the calibration dataset. The rationale behind this simplification is that u_c and D characterize the migration of a flood wave that strongly depends on channel geometry and streamflow magnitude (Beven, 2020). Because storm duration and intensity are closely related to streamflow magnitude, it is reasonable to expect a functional dependence between the model parameters u_c and D and the storm duration and intensity. Once the surrogate models for u_c and D are defined, we used the following procedure to validate the Directional-UH model:

- 1. A storm catalog of moving storm events is created for validation. This storm catalog was created using 144 moving storm events based on the combination of rectangular storm parameters with $D_s \in [1,3,6,12,24,48,72]$ h, RC=0.2, $i_s \in [5,10,15]$ mm/h, $v_s \in [1,2,5,10,15,20]$ m/s, and $\theta_s = 0^{\circ}$.
- Hydrographs resulting from the previous storm catalog are calculated with the HLM model and the Directional-UH model. The model parameters for the Directional-UH model are calculated using surrogate models from the calibration procedure.

Note that the surrogate models for u_c and D are constructed from stationary storm events. Therefore, validating whether such equations can be used for rectangular moving storms is critical for implementing the Directional-UH model.

4.4. Evaluation of hydrologic system dynamics

Once the Directional-UH model is calibrated and validated, we conducted systematic simulations to understand and quantify the effect of storm velocity (speed and direction) and storm structure in peak flow magnitude. We focus our analysis on three main components. First, we identify the storm trajectory that maximizes the peak flow response. To this end, we quantify peak flows by predefining synthetic moving

storms with storm intensities associated with a 10-year return period and storm directions ranging from 0° to 350° with a 10° interval. Ideally, and similar to the extraction of Watershed-IDF curves, radar rainfall observations could be used to estimate the Intensity-Duration-Velocity-Frequency (IDVF) curves associated to a rectangular moving storm, where a new dimension, storm speed, is added to estimate rainfall intensity in a rectangular moving block as a function of storm duration, storm velocity, and probability of recurrence. Unfortunately, estimating IDVF curves is an unexplored field, and IDVF curves are not available. To address this situation, we used the watershed-IDF curves extracted from RainyDay (Wright et al., 2017) as a proxy of the IDVF curves to define the rainfall intensities in the rectangular storm associated to a 10-year return period. Note that another option to define the storm intensity, i_s , is to use Point-IDF estimates, such as those offered by Atlas-14 (Bonnin et al., 2006). This, however, requires us to use area reduction factors to account for the reduction of average rainfall intensities as the watershed area increases. The use of Point-IDFs with area reduction factors do not necessarily capture the average intensities observed from distributed rainfall datasets (Wright et al., 2014; Kim et al., 2019). As a result, when possible, we recommend using the Watershed-IDF extracted from gridded rainfall datasets such as those provided by RainyDay (Wright et al., 2017). We envision future studies focusing on estimating IDVF curves to be implemented in the Directional-UH model.

The second analysis focuses on the effect of storm speed on peak flow magnitude. This was done by exploring the emergence of resonance conditions, which we define as the conditions when the combined effects of storm motion and flood wave migration maximize the peak flow response. For this purpose, we use the Directional-UH to find the combination of v_s and θ_s that maximizes the peak flow response for given values of i_s and D_s . Finally, the third analysis focuses on the effect of compound storm events on flood generation. To this end, we evaluate the peak flow dynamics resulting from two consecutive storm events separated by a time window Δt . We show that the Directional-UH model can easily be used to systematically evaluate compound storm trajectories between two independent storm events. This is of particular interest for analyzing peak flow dynamics in large river basins, where flood events are commonly the result of compound storm events.

5. Results and discussion

5.1. Transformation to rectangular storm events

We selected 273 storm events from the 350 detected by RainyDay. The selected events have the highest accumulated rainfall and welldefined storm cores, allowing us to characterize the motion of the main storm core. The remaining 77 storms have the lowest accumulated rainfall with scattered spatial patterns of intensity and without welldefined storm cores. We estimated the parameters v_s , θ_s , D_s , and i_s for each of these 273 storm events (see Fig. 5C-G). Then, based on these average storm characteristics (see Appendix), each observed storm was transformed into its equivalent rectangular moving storm representation (e.g., Fig. 5A, B). We found that v_s ranges from 0.8 to 20 m/s, with a mean value of 4.2 m/s, and a standard deviation of 2.8 m/s (Fig. 5C). The i_s ranges from 5.9 to 15.8 mm/h, with a mean value of 9.1 mm/h and a standard deviation of 1.9 mm/h (Fig. 5D). The D_s ranges from 1 to 95 h, with a mean value of 18 h and a standard deviation of 14 h (Fig. 5F). In this case, D_s was calculated as the pairwise ratio of w_s (Fig. 5H) and v_s (Fig. 5C). This means that although the storm catalog was extracted from a time window of 72 h, very low values of v_s in combination with large values of w_s may provide D_s values longer than 72 h. Consistent with previous empirical analyses (Perez et al., 2021; Prein et al., 2020), storm cores travel preferentially with an east to west path (histogram modes near $\bar{\theta}_s = 0^{\circ}$ or $\bar{\theta}_s = 360^{\circ}$); however, we observed storms across the full spectrum of direction, they just occur less frequently (Fig. 5G).

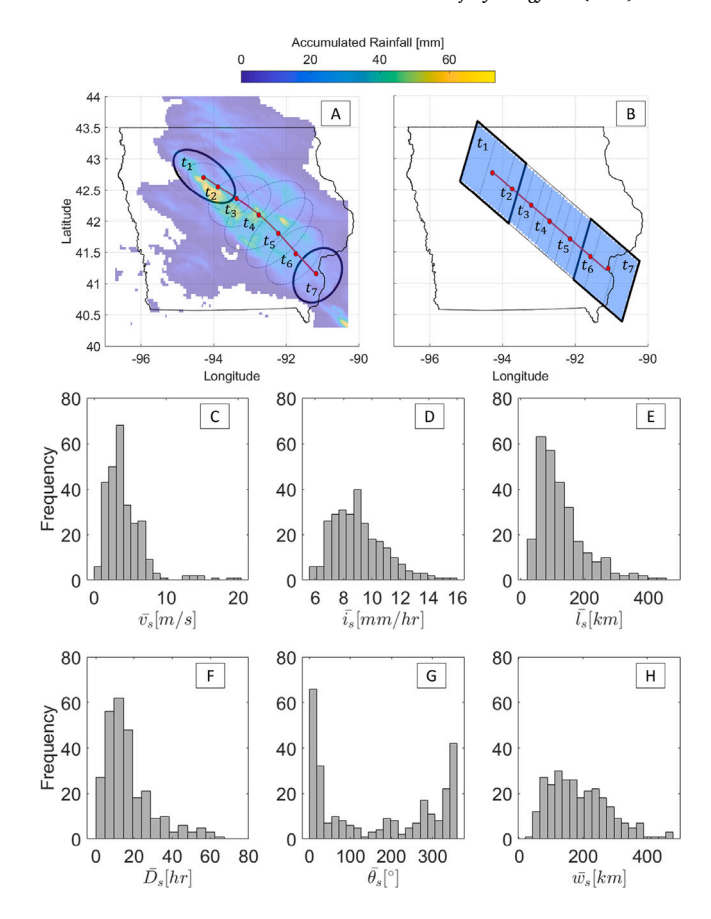


Fig. 5. Example of the transformation from an observed storm event (A) to a rectangular moving storm (B). The storm in panel A is from August 9, 2006, 08:00:00 to August 9, 2006, 14:00:00 GMT+0000. Histograms for $\bar{v_s}$ (C), $\bar{I_s}$ (D), $\bar{D_s}$ (E), $\bar{\theta_s}$ (F), $\bar{I_s}$ (G), and $\bar{w_s}$ (H). The histograms are calculated using 273 storm events. We use a bar in the variable names to indicate that these values were estimated from observations.

Regarding the spatial extent of the storms, the Directional-UH model assumes l_s is larger than the diameter of the circumscribed circle of the watershed. As a result, it is important to quantify how many of the observed storm events can satisfy this condition. The diameter of the circumscribed circle of the Turkey River boundary is 145 km, which is comparable with the median \bar{l}_s value of 106 km (Fig. 5E). With this diameter, about 30% of the observed storm events have the potential to completely cover the Turkey River watershed for any storm direction. However, it should be noted that the exact l_s required to cover the entire basin depends on the storm direction. For example, when $\theta_s = 45^{\circ}$ or $\theta_s = 225^{\circ}$, l_s must be larger than 145 km to cover the watershed domain. On the other hand, when $\theta_s = 160^{\circ}$ (storm moving in the downstream direction) or $\theta_s = 340^{\circ}$ (storms moving in the upstream direction), an l_s of 45 km is sufficient to cover the entire watershed. When we consider this directional dependence, about 95% of the observed storm events satisfying this the Directional-UH model assumption.

To the best of our knowledge, this is the first study to propose a coherent framework to transform observed storm events into rectangular events for the efficient simulation of rainfall-runoff response. Our procedure (see Appendix) assumes a relatively simple representation of shape and intensity to satisfy the assumptions behind the current version of the Directional-UH model. However, future implementations could relax this assumption to improve the spatiotemporal representation of the storm events, for example, by including multiple storm blocks of varying intensities.

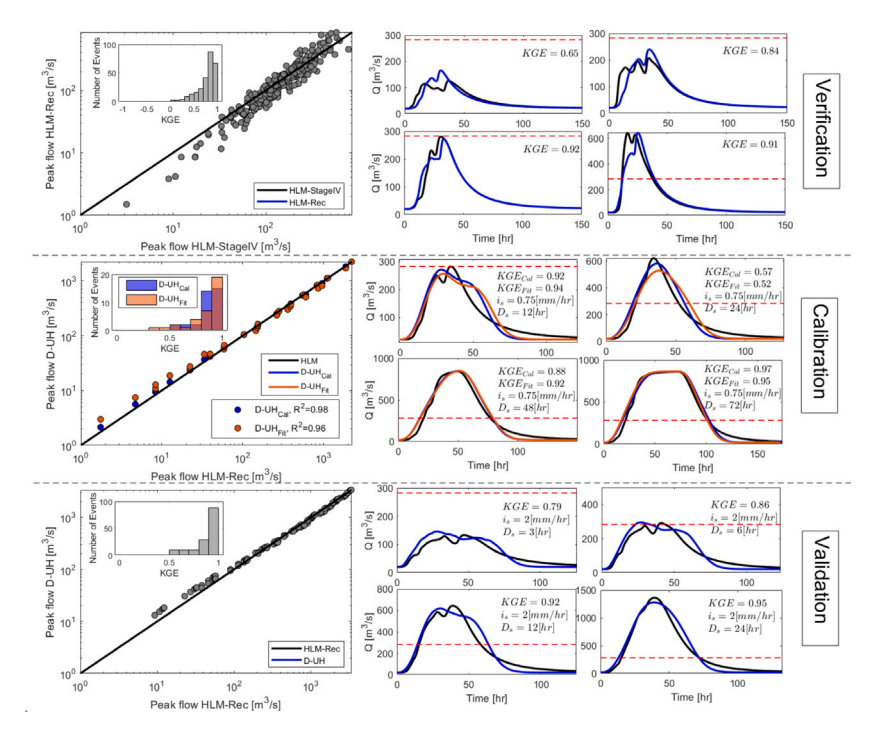


Fig. 6. Verification, calibration, and validation of the Directional-UH model. The scatter plot in the verification panel compares peak flows estimated from the HLM model using the rainfall dataset Stage-IV (Peak flow HLM-StageIV) versus equivalent rectangular moving storms (Peak flow HLM-Rec). 273 storm events selected from 2002 to 2020 were used for the verification, with peak flows ranging from 3 to 780 m³/s. Four arbitrarily selected hydrographs from Stage-IV and equivalent rectangular moving storms are presented in the verification panel. The scatter plot in the calibration panel compares peak flows from stationary storms using the HLM model (Peak flow HLM-Rec) against the Directional-UH model (Peak flow D-UH). The blue hydrographs (D-UH_{cal}) are obtained by calibrating u_c from the HLM hydrograph. The red hydrographs (D-UH_{fil}) are obtained by estimating u_c based on the regression Eq. (18). A total of 35 synthetic stationary storm events are used in the calibration process, with peak flows ranging from 2 to 2250 m³/s. The scatter plot in the validation panel compares peak flows resulting from moving rectangular storms using HLM (Peak flow HLM-Rec) and the Directional-UH (Peak flow D-UH). 144 rectangular moving storms are used in the validation process, with peak flows ranging from 9 to 3400 m³/s. (For interpretation of the references to color in this figure legend, the reader is referred to the web version of this article.)

5.2. Verification, calibration, and validation

To verify the validity of our rectangular storm representation, we compare peak flows obtained from HLM simulations forced with observed rainfall events and their equivalent rectangular representation (see the Verification panel in Fig. 6). Hydrological model performance can be conducted using various approaches (e.g., Burgan and Aksoy, 2022). In our study, we assess model performance using the Kling-Gupta efficiency (KGE) performance metric, where KGE values of one indicate perfect correspondence between simulations and reference values, and values close to zero mean that the model simulations have the same explanatory power as the mean of the reference values. Overall, the results show that the rectangular storm assumption is a reasonable representation to capture the streamflow dynamics from observed rainfall events, with 95% of the storm events having a KGE value greater than 0.8.

The agreement between hydrographs resulting from rectangular storms and observed storms suggests that total rainfall amounts (encapsulated in i_s , w_s , and l_s) and the storm motion characteristics (encapsulated in v_s and θ_s) are first-order controls for the peak flow response at the scale of the Turkey River watershed. At this scale, the spatial variability in storm cores is likely to play a less dominant role in the peak flow response (Zhu et al., 2018; Singh, 1997). We hypothesize that the spatial variability in storm cores will play a more significant role in shaping peak flow response for smaller watershed scales. Therefore rectangular moving storms will likely introduce biases in their estimates. It is important to note the presence of other confounding factors that could be important in assessing the rectangular storm assumption. For example, the benchmark model used in this study, the HLM model, uses a constant runoff coefficient, limiting our ability to assess the role of spatial variability of subsurface processes and antecedent soil moisture conditions. While this is out of our scope, future

applications can increase the complexity of the model to fully assess the strengths and limitations of the rectangular storm conceptualization.

For individual stationary storm events, the Directional-UH model with calibrated parameters u_c and D replicates the hydrographs from the reference model HLM (see Fig. 6, Calibration panel). We found that for a stationary storm event the following expression can be used to estimate the expected channel celerity, $u_{\bar{c}}$ (in m/s), as function of the storm effective intensity, i_e (in mm/h), and storm duration, D_s (in hours).

$$\bar{u}_c = 0.5947 \, i_e^{0.3717} \, D_s^{0.2737}. \tag{18}$$

Eq. (18) was fitted in logarithmic space, and the linear regression has a $R_{adi}^2 = 0.94$ and a RMSE = 0.13 m/s. We found that the dispersion coefficient D was insensitive to the rainfall characteristics i_e and D_s ; therefore, we define D as equal to 1 m²/s for all simulations. Because D introduces a smoothing effect, its impact will be more prominent in systems smaller than the Turkey River watershed. In particular, Eq. (18) states that for a stationary storm event of a duration of one hour and an effective rainfall intensity of one millimeter per hour, the average value of u_c is 0.59 m/s. It can also be observed from Eq. (18) that the exponent related to i_s is 0.37, and for D_s is 0.27, this means that u_c increases more rapidly with increasing i_s than D_s . Finally, we remark that Eq. (18) captures the hydrodynamics embedded within the HLM model and is only valid for the analysis of the flow at the outlet of the Turkey River watershed. From a broader perspective, similar regression analyses for a diverse set of watershed scales and hydrological domains will be critical to facilitate the implementation of unit hydrograph models when streamflow observations are not available for model calibration.

Regarding the validation of the Directional-UH model, we found that the Directional-UH model with u_c estimated from Eq. (18) can reproduce the streamflow response from the reference model HLM. In

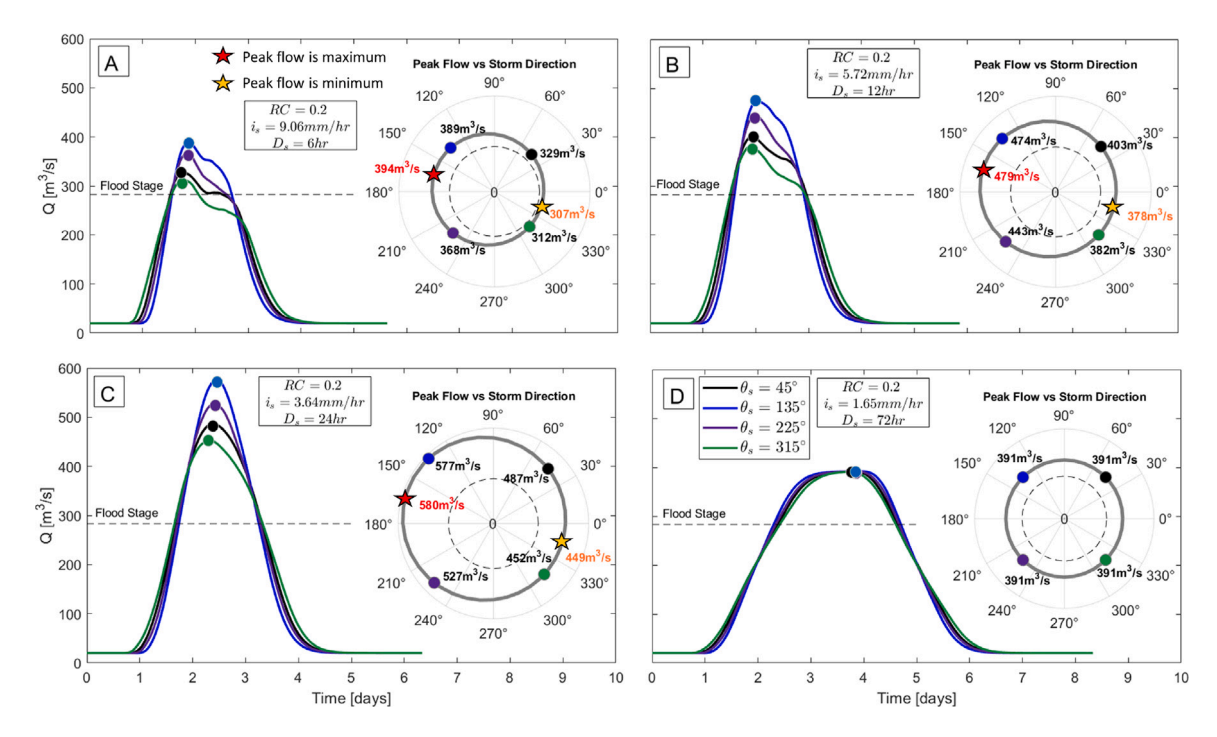


Fig. 7. Hydrographs obtained from the Directional-UH using a storm speed $v_s = 5 \,\mathrm{m/s}$ and different values of storm direction, θ_s , storm duration, D_s , and storm intensity, i_s . The storm duration and storm intensity are defined based on the 10-year return period defined from the Watershed-IDF curve obtained from the Stage-IV radar rainfall dataset and RainyDay. The circular plot on each panel depicts the peak flow magnitude (radius) as a function of the storm direction (angle), θ_s . The effective storm intensity, i_e is calculated by assuming a spatially uniform runoff coefficient of 0.2. The red start indicates the storm direction where the peak flow is maximum. Note that in panel D, the peak flow is independent of the storm direction because the storm duration is larger than the basin hydrologic response time. (For interpretation of the references to color in this figure legend, the reader is referred to the web version of this article.)

particular, most of the rainfall-runoff event simulations have a KGE higher than 0.5 (see Fig. 6, Validation panel). This agreement for moving storms is a significant result that highlights the potential of our parsimonious approach to capture complex storm structure and velocity patterns, especially considering that Eq. (18) was constructed from stationary storm events.

In summary, the verification, calibration, and validation results demonstrate that the Directional-UH model reasonably approximates the reference model HLM for rainfall-runoff simulations in the Turkey River watershed. Therefore, the Directional-UH model can be used as an effective tool to systematically explore the effect of storm properties such as storm direction and speed in peak flow magnitude.

5.3. Connecting peak flow response to storm dynamics

5.3.1. Critical storm trajectories

We use the Directional-UH model to identify the critical storm direction that maximizes peak flow response for the Turkey River watershed. To this end, the system was forced by moving rectangular storms with 6, 12, 24, and 72 h duration and rainfall intensities extracted from the Watershed-IDF associated with a 10-year return period (Wright et al., 2017). In addition, the storm speed was set to $5\,\text{m/s}$, which is close to the average velocity of $4.2\,\text{m/s}$ estimated from the observed storms (Fig. 5C), and $l_s=145\,\text{km}$ was used for all simulations (Fig. 5E) to satisfy the assumption of the Directional-UH model.

The results of this numerical experiment are summarized in Fig. 7. In this case, peak flows are shown as a function of storm direction θ_s using circular plots, where the angle represents θ_s , and the radius represents the peak flow magnitude. For the storm events of 6, 12, and 24 h, the peak flow magnitude reaches a maximum when the storm travels in the downstream direction ($\theta_s \approx 160^\circ$) and a minimum when the storm travels in the upstream direction ($\theta_s \approx 340^\circ$). This relationship between storm trajectory and basin orientation is well documented in the literature (Smart and Surkan, 1967; Foroud et al.,

1984; Ngirane-Katashaya and Wheater, 1985; Watts and Calver, 1991; Singh, 1997, 2002; Perez et al., 2021). The smooth oval pattern for the peak flow magnitude in Figs. 7A-C are explained by the predominant orientation of the Turkey River network that flows in the southeast direction. However, we hypothesize that for watershed systems where the main river stem has abrupt changes in river orientation along the watershed (e.g., in an L-shaped watershed, with the upstream network draining from north to south and the downstream section draining from west to east), irregular patterns will emerge. Finally, the magnitude of the peak flow also depends on the storm's duration, intensity, and speed (Singh, 1997). Therefore, storm trajectories along the main axis of the watershed do not always coincide with the minimum and maximum peak flows. For example, peak flow is independent of storm direction for the 72-h storm duration (Fig. 7D).

For the Turkey River watershed, we summarize some key points on the relation between storm motion and peak flow magnitude. (i) With increasing D_s , the effect of θ_s on peak flow decreases. For instance, the storm motion becomes irrelevant for a long-duration storm event, similar to a stationary storm event. (ii) With increasing v_s , the effect of θ_s on peak flow decreases. From a physical perspective, at high v_s values (e.g., $20\,\text{m/s}$), rainwater is delivered along the watershed faster than the speed at which water moves in hillslopes and channels (e.g., u_c around $2\,\text{m/s}$). (iii) Peak flow is maximum when the storm travels in the downstream direction parallel to the main river channel. (iv) Peak flow is minimum when the storm travels in the upstream direction. And (v) when the storm travels in the downstream direction, there is a resonance effect once the v_s equals to the flood wave speed (Volpi et al., 2013).

The parsimony of the Directional-UH model allows us to investigate the patterns described above in detail and with a reasonable computational burden. Fig. 8 summarizes hundreds of numerical experiments used to explore the parameter space D_s , v_s , and θ_s . In these figures, we describe peak flow as a function of v_s and D_s for different θ_s values when $i_s=9.65\,\mathrm{mm/h}$ and a RC=0.2. Furthermore, to aid

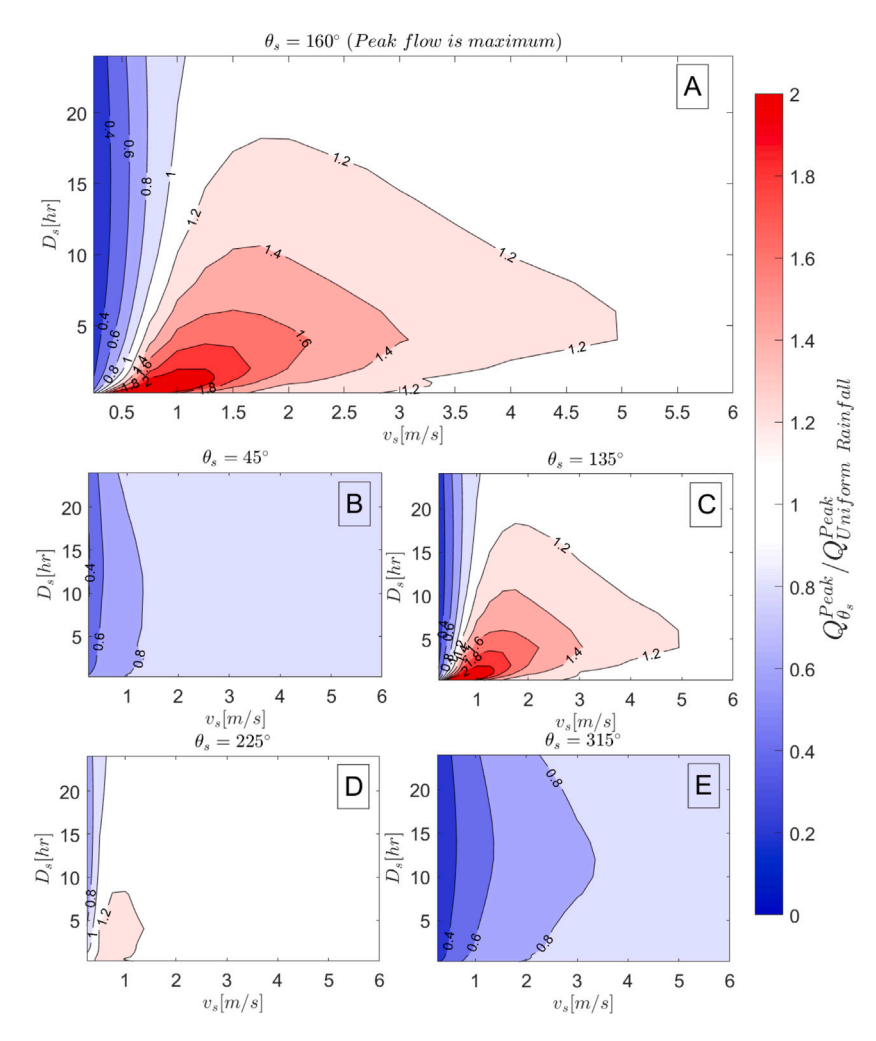


Fig. 8. Scaled peak flow for different storm directions, θ_s , as a function of storm speed, v_s , and storm duration, D_s . The peak flow is scaled by the peak flow that would result from a stationary storm event. Red colors correspond to cases where peak flow is underestimated by assuming stationary storms. Blue colors correspond to cases where peak flow is overestimated by assuming stationary storms. All simulations assume a storm intensity of 9.65 mm/h and a runoff coefficient of 0.2. (For interpretation of the references to color in this figure legend, the reader is referred to the web version of this article.)

interpretation, peak flows are normalized by the peak flow resulting from a stationary storm with the same rainfall intensity and duration. In other words, values near one correspond to cases where the storm motion properties (v_s and θ_s) do not significantly affect the magnitude of peak flows. In contrast, values larger (smaller) than one represent conditions where the peak flow magnitude is higher (lower) than expected when the system is forced by a stationary storm, highlighting the conditions where storm dynamics plays a critical role in the peak flow magnitude.

When $\theta_s=160^\circ$ (Fig. 8A), we found significant fractions of the parameter space v_s and D_s that result in peak flows higher (red areas) and lower (blue areas) than the peak flow resulting from a stationary storm. A similar behavior is seeing for $\theta_s=135^\circ$ (Fig. 8C). Now, when $\theta_s=315^\circ$ or $\theta_s=45^\circ$, which are values close to angles that minimize peak flow ($\theta_s=340^\circ$), the whole parameter space is characterized by peak flow values lower than one (blue areas) (Fig. 8B,E). Finally, for $\theta_s=225^\circ$, most of the parameter space results in peak flow magnitudes similar to the ones obtained with a stationary storm (white areas in Fig. 8D).

The previous results are particularly relevant to identify the conditions for which using a stationary storm provides a reasonable estimate of the peak flow response. Similarly, the results serve as a reference to identify conditions that will lead to overestimation or underestimation of peak flow magnitudes due to misrepresentation of storm structure.

5.3.2. Resonance conditions for hydrologic response

Spatiotemporal synchrony between the flood wave and the storm core amplifies the hydrologic response, significantly increasing peak flow magnitude (Ngirane-Katashaya and Wheater, 1985). This synchronization can happen when the storm travels along the main river direction at a speed comparable with the flood wave. Here, we refer to this condition as *resonance*. Previous studies had focused on quantifying peak flow magnitudes for resonance conditions (Volpi et al., 2013; Seo et al., 2012; Ghimire et al., 2021). In particular, the propagation of the flood wave (characterized by channel celerity) depends on the channel discharge, which also depends on the effective rainfall intensity. This correlation means that the occurrence of resonance also depends on the rainfall intensity and antecedent soil moisture conditions.

As a proof of concept, we use the Directional-UH model to explore the genesis of resonance conditions in the Turkey River watershed. In this case, we find the storm speed (v_s) that equals the channel flow celerity (u_c) for a given storm duration (D_s) and effective intensity (i_s) . For instance, for a $D_s=5$ h and $i_s=1.85$ mm/h, the storm speed that maximizes peak flow response is $v_s=1.3$ m/s (Fig. 8A). This speed is close to the channel flow celerity $u_c=1.15$ m/s obtained from Eq. (18). Note that for this case, the resonance condition has the potential to increase by a factor of 2 the peak flow magnitude when compared to stationary storm events. The Directional-UH model can identify storm characteristics, particularly v_s and θ_s , resulting in a resonance condition.

Although resonance conditions are plausible in hydrological systems, their probability of occurrence is expected to be relatively low, given the number of concurrent conditions needed. As a taught experiment to illustrate the likelihood of extreme resonance conditions, we will explore events with a 500-years return period, which serves as a proxy for the most extreme storm events occurring in the Turkey River watershed. In this case, we use the Watershed-IDF (Wright et al., 2017) to estimate the storm intensities for durations ranging from 1 to 72 hours. These intensities are then converted to effective intensities assuming a runoff coefficient of 0.8, mimicking the high soil moisture content conducive to an extreme flood response. Then, using the resulting (i_s, D_s) pairs and Eq. (18), we predict that a maximum channel celerity $u_c = 2.6 \,\text{m/s}$ would occur for $D_s = 24 \,\text{h}$ and $i_s = 7.24 \,\text{mm/h}$. Therefore, for these conditions, only storms with v_s less than 2.6 m/s could resonate with the flood wave, assuming that also D_c and i_c are in the adequate ranges. From the observed storm events (Fig. 5C), about 30% of the events meet this condition.

From a practical perspective, quantifying how far or close the hydrological and meteorological conditions are from the resonance conditions is critical to our interpretations of physical mechanisms leading to extreme hydrologic response. For instance, storm patterns observed from the Stage-IV dataset from 2002-2020 show that all storm directions in the state of Iowa could meet the resonance requirements (Fig. 5G), with preferential storm directions from west to east (with $\bar{\theta}_{\rm s} \approx 0^{\circ}$). Connections between the distribution of the frequency of storm directions observed from rainfall datasets and their control on flood generation can provide information on the processes shaping extreme peak flows, particularly heavy tails of peak flow distributions (Merz et al., 2022). We hypothesize that extreme flood responses shaping the right tail of the peak flow distribution could result from storms traveling along critical trajectories. Furthermore, exploring the entire spectrum of peak flows resulting from all directions provides a fundamental basis for understanding and quantifying the potential effects of shifts in storm trajectories driven by changes in atmospheric patterns. For example, most flood events in the Turkey River watershed are mainly the result of storms coming from the preferential direction $\theta_s \approx 0^{\circ}$. Then, using the circular plots in Fig. 7, we infer that a counterclockwise shift of storm directions in the region will produce an increase of peak flow magnitudes and, on the contrary, shifts in a clockwise direction will cause the peak flows to decrease.

5.3.3. Compound storm events

Peak flows resulting from consecutive storm events are one of the leading causes of catastrophic flood events (Smith et al., 2013). Two mechanisms can explain the intensification of peak flows by consecutive storm events. First, the initial storm event increases the antecedent soil moisture conditions, and as a result, later rainfall events produce larger runoff amounts. Second, although the runoff signature for each storm event can differ in space and time, the runoff can be aggregated along the river network. An example of this aggregation effect is the case of an initial storm producing runoff in the upstream region of a watershed followed by a later storm in the downstream area. The runoff response from these events results in an amplified signal (see, for an example, simulations in Perez et al., 2021).

Identifying the characteristics of two or more storm events (compound storms) that lead to the most extreme peak flow response is not a trivial problem because of the countless combinations of storm characteristics that can result in an extreme hydrologic response. In other words, exploring all the possible combinations of storm intensities, durations, speeds, and directions between two or more events can result in an untractable computational problem. Here, we tackle this problem with the Directional-UH model, taking advantage of the linearity of the model, which in turn allows us to use the superposition principle to calculate the hydrograph resulting from consecutive storm events separated by a time Δt_{Storm} .

To illustrate this analysis, we conducted systematic rainfall-runoff simulations to calculate the peak flow resulting from two consecutive storm events (storm 1 and storm 2) separated by a time Δt_{Storm} of 1, 6, 12, and 24 h. For simplicity, we assume the first storm event is characterized by $i_s=31.24\,\mathrm{mm/h},\ D_s=1\,\mathrm{h},\ v_s=5\,\mathrm{m/s},\ \theta_s=320^\circ,$ and a RC=0.2. The second event, which arrives a Δt_{Storm} time later than storm 1, is characterized by $i_s=4.82\,\mathrm{mm/h},\ D_s=12\,\mathrm{h},\ v_s=5\,\mathrm{m/s},\ \theta_s=90^\circ,$ and a RC=0.3. For storm 2, we used a higher runoff coefficient to reflect the increase in soil moisture content caused by storm 1.

The peak flows from all possible combinations of storm direction are presented in Fig. 9D-G. These results allow us to identify critical combinations between two storm trajectories that maximize peak flow. In particular, because storm 2 is the event that produces the highest individual peak flow response (green hydrograph in Fig. 9C), $\theta_s = 160^{\circ}$ is consistently the critical storm trajectory for storm 2 independent of Δt_{Storm} . On the other hand, because storm 1 produces the lower individual peak flow, the critical θ_s for storm 1 with the maximum value of the compounded peak flow varies with Δt_{Storm} . For instance, for $\Delta t_{Storm} = 1$ h, the maximum peak flow occurs for the combination of $(\theta_{Storm1} = 160^{\circ}, \theta_{Storm2} = 160^{\circ})$, for $\Delta t_{Storm} = 6 \, \text{h}$ the critical angles are $(\theta_{Storm1} = 150^{\circ}, \theta_{Storm2} = 160^{\circ})$, for $\Delta t_{Storm} = 12 \, \text{h}$ the critical angles are $(\theta_{Storm1} = 140^{\circ}, \theta_{Storm2} = 160^{\circ})$, and for $\Delta t_{Storm} = 24 \, \text{h}$ the critical angles are $(\theta_{Storm1} = 340^{\circ}, \theta_{Storm2} = 160^{\circ})$. To summarize, although the critical trajectory of $\theta_s = 160^{\circ}$ dominates the highest peak flow magnitude from a single storm event in the Turkey River watershed, this analysis of compound storm events demonstrates that other storm trajectories are critical to correctly identify potential combinations that lead to the most extreme flood events.

In this systematic analysis, the two storms we used were designed for illustrative purposes. However, a deep understanding of the compounding effects of consecutive storms in peak flow response will require a more exhaustive analysis, including larger combinations of storm intensities, durations, and velocities. We envision future applications of the Directional-UH model where compounding storm effects are evaluated with catalogs of storm structures that resemble possible combinations from radar rainfall datasets.

Analyzing consecutive storm events to understand flood genesis is critical for large river basins. Along these lines, the storm conditions prescribed by the Directional-UH model are unlikely to occur in large river basins because rainfall intensities within storm cores are likely to change drastically across long trajectories, and the size of the storms will be small compared to the modeling domain, violating two of the fundamental assumptions behind our approach. However, as described in Section 3, the Directional-UH model can be modified to account for smaller storms and spatially variable storm intensity. Overall, although the increase in spatial heterogeneity and possible flow controls (e.g., dams and reservoirs) in large river basins prevents the implementation of the current version of this parsimonious framework, future modifications to the Directional-UH model can overcome these limitations and become a valuable tool to address the longstanding and challenging problem of flood prediction in large river basins.

6. Conclusions

This study introduced the Directional-UH model, a parsimonious hydrological model, to assess the effect of storm structure and velocity on hydrograph response. This model simplifies storm fields into rectangular moving storms, incorporating storm shape, speed, and direction into the instantaneous unit hydrograph function. We called this new function the Instantaneous Directional Unit Hydrograph (IDUH). The IDUH represents the streamflow response due to an instantaneous unitary intensity pulse from a rectangular storm moving with constant speed, v_s , along a linear trajectory described by the storm direction, θ_s .

The verification, calibration, and validation conducted in the Turkey River watershed demonstrated that the Directional-UH model can

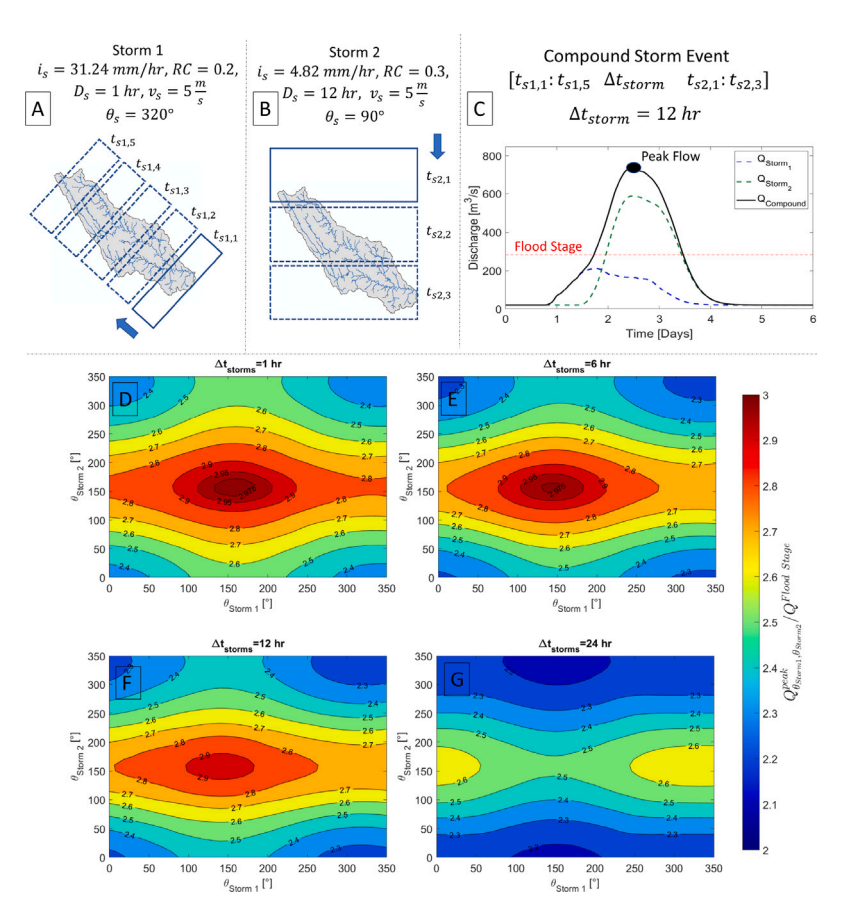


Fig. 9. Example of the hydrological response (C) resulting from the interaction between Storm 1 (A) and Storm 2 (B) separated by a time interval Δt_{storm} . Normalized peak flow surfaces resulting from the combinations of Storm 1 and Storm 2 for different directions with a time interval Δt_{storm} of 1 h (D), 6 h (E), 12 h (F), and 24 h (G). The peak flows are normalized with respect to the flood stage magnitude of 283 m³/s reported by the USGS.

reproduce rainfall-runoff responses similar to those estimated from observed radar rainfall fields. Although flood dynamics results from complex hydrological processes that are evolving in space and time and do not come from ideal rainfall simplifications, our results prove that the Directional-UH model can be a valuable tool to analyze peak flow dynamics by systematically varying storm characteristics.

The parsimonious nature of the Directional-UH model allows us to explore complex problems with minimal computational burden. For example, the tool can be used to

- Identify the critical storm trajectory that maximizes peak flow magnitude.
- Establish the storm characteristics leading to resonance conditions. That is when synchrony between the storm motion and the flood wave creates the most extreme peak flow response.
- 3. Determine the implications for runoff response of approximating moving storm events with equivalent stationary ones.
- Quantify the changes in peak flow magnitudes caused by shifts in storm trajectories.
- 5. Identify the combination of consecutive storm events that create the most extreme peak flow response.

From a mechanistic perspective, the Directional-UH model can characterize the well-established relationship between storm motion characteristics and peak flow dynamics. This relationship was illustrated for our testbed, the Turkey River watershed. For this system, we found that (i) with increasing storm duration, the effect of storm direction on peak flow diminishes, with no discernible effect for storm durations exceeding three days; (ii) with increasing storm velocity, the effect of the storm direction on peak flow decreases, with no discernible effect for storm velocities exceeding 6 m/s; (iii) the peak flow is maximum

when the storm travels in the downstream direction (160° measured in a counterclockwise direction from the east–west axis) parallel the main river channel; (iv) the peak flow is minimum when the storm travels in the upstream direction (340°) parallel to the main river channel; and (v) when the storm travels in the downstream direction and the storm velocity is equal to the flood wave, there is a resonance effect that has the potential to increase the peak flow magnitude by a factor of two when compared to a stationary storm.

The Directional-UH model, as developed and implemented in this study, assumes rectangular moving storms of constant intensity forcing a watershed with a spatially uniform runoff coefficient. We demonstrate that the current version of the model captures the hydrologic response for the testbed scenarios explored. However, these assumptions can be relaxed further to improve the mechanistic fidelity of the Directional-UH model. Future improvements on the Directional-UH model are expected to provide a broader array of storm characteristics, encompassing:

- 1. Spatial variable runoff coefficients,
- 2. Variable rainfall intensity in the rectangular storm, and
- Partial storm coverage.

The flexibility of the Directional-UH model makes it a hydrological tool with the potential to expand our interpretations of rainfall-runoff dynamics and shape our engineering practices by improving peak flow estimations while accounting for essential storm characteristics such as storm structure, direction, and speed. Furthermore, storm characteristics will likely change under future climate, making parsimonious tools such as the Directional-UH model more pertinent to guide engineering practices for adaptation and flood preparedness.

CRediT authorship contribution statement

Gabriel Perez: Conceptualization, Methodology, Software, Validation, Formal analysis, Investigation, Writing – original draft. Jesus D. Gomez-Velez: Conceptualization, Methodology, Writing – review & editing, Project administration, Funding acquisition. Xingyuan Chen: Validation, Project administration, Writing – review & editing. Timothy Scheibe: Validation, Project administration, Writing – review & editing.

Declaration of competing interest

The authors declare that they have no known competing financial interests or personal relationships that could have appeared to influence the work reported in this paper.

Data availability

The scripts to implement the Directional-UH are publicly availale at https://github.com/gomezvelezlab/Directional-UH.

Acknowledgments

This research was funded by the U.S. Department of Energy, Office of Science, Biological and Environmental Research. This work is a product of two programs: (i) Environmental System Science Program, as part of the River Corridor Scientific Focus Area project at Pacific Northwest National Laboratory, the Watershed Dynamics and Evolution (WaDE) Science Focus Area at Oak Ridge National Laboratory, and the IDEAS-Watersheds project, and (ii) Data Management Program, as part of the ExaSheds project. Additional support was provided by the National Science Foundation, USA (awards EAR-1830172, OIA-2020814, and OIA-2312326). This research used resources of the Compute and Data Environment for Science (CADES) at the Oak Ridge National Laboratory, which is supported by the Office of Science of the U.S. Department of Energy under contract no. DE-AC05-00OR22725. Oak Ridge National Laboratory is managed by UT-Battelle, LLC, for the DOE under contract no. DE-AC05-00OR22725. The scripts to implement the Directional-UH are publicly available at https://github.com/ gomezvelezlab/Directional-UH.

Appendix. Procedure for estimating equivalent rectangular storm parameters

The TITAN storm tracking algorithm (Dixon and Wiener, 1993) with the object-based storm identification algorithm presented by Li et al. (2020) is used to identify the storm trajectory and storm properties at each time step for the 350 storm events detected by RainyDay. In particular, this algorithm can detect multiple storm cores in a given time, t. For a given t, we focused on the main storm core with the highest intensity, and limit our analysis to storm events that display spatially congruent storm cores of at least 4 h of development. We conducted a visual verification of each storm track to remove storm events distorted by artifacts caused by radar measurements. This last condition filtered the number of events to 277 storm events. The transformation of an observed storm event into a rectangular moving storm was conducted as follows:

- 1. The geometry of the main storm core at each time, t, is extracted from the storm tracking algorithm. The main storm core geometry consists of an ellipse with orientation α_t [°], with a major axis, R_t [L], a minor axis, r_t [L], and with a center point with coordinates $(x_{c,t}, y_{c,t})$.
- 2. The average linear direction, $\bar{\theta_s}$, and the linear trajectory of the moving storm are estimated from a regression line using the center points $(x_{c,t}, y_{c,t})$.

3. The average storm velocity is estimated from the change in position of the center points $(x_{c,t}, y_{c,t})$ during the storm event. Therefore, the average storm velocity \bar{v}_s is calculated as

$$\bar{v_s} = \frac{1}{N-1} \sum_{t=1}^{N-1} \sqrt{(x_{c,t+1} - x_{c,t})^2 + (y_{c,t+1} - y_{c,t})^2} / \Delta t$$
 (A.1)

where Δt [T] is the time resolution of the storm event, and N [-] is the number of time steps within the storm event.

- Each ellipse, at each time t, is transformed into a rectangle with sides R_t and r_t preserving the same orientation α_t.
- 5. Each side R_t and r_t are categorized and redefined as a parallel side $(Side_{t,\parallel}\ [L])$ or perpendicular side $(Side_{t,\perp}\ [L])$ depending on its relative orientation to the linear storm trajectory.

$$Side_{t,\parallel} = \begin{cases} R_t & R_t \text{ is the side closer to a parallel orientation to} \\ r_t & r_t \text{ otherwise} \end{cases}$$

(A.2)

 $Side_{t,\perp} = \begin{cases} R_t & R_t \text{ is the side closer to a perpendicular orientation to} \\ & \text{the linear storm trajectory} \\ r_t & r_t \text{ otherwise} \end{cases}$

(A.3)

6. The sides $Side_{t,\parallel}$ and $Side_{t,\perp}$ at each time step t are used to estimate an unique equivalent rectangle with sides

$$\bar{w_s} = \frac{1}{N} \sum_{t=1}^{N} Side_{t,\parallel}$$
 (A.4)

$$\bar{l}_s = \frac{1}{N} \sum_{t=1}^{N} Side_{t,\perp}$$
 (A.5)

7. The intensity, \bar{l}_s , of the rectangular storm event is calculated so that the rainfall accumulation by the rectangular moving storm matches the total accumulated precipitation, $P_{s,T}$ [L], that is observed in the basin from the radar rainfall dataset. This is done by

$$\bar{l_s} = P_{s,T} \frac{\bar{v_s}}{i\bar{v_s}} \tag{A.6}$$

References

Andrieu, H., Moussa, R., Kirstetter, P.-E., 2021. The Event-specific Geomorphological Instantaneous Unit Hydrograph (E-GIUH): The basin hydrological response characteristic of a flood event. J. Hydrol. 603 (November), 127158.

Aron, G., White, E.L., 1982. Fitting a Gamma distribution over a synthetic unit hydrograph. J. Am. Water Resour. Assoc. 18 (1), 95–98.

Bernard, M.M., 1935. An approach to determinate stream flow. Trans. Am. Soc. Civ. Eng. 100 (1), 347–362.

Beven, K., 2020. A history of the concept of time of concentration. Hydrol. Earth Syst. Sci. Discuss. 1–28.

Bhunya, P., 2011. Synthetic unit hydrograph methods: A critical review. Open Hydrol. J. 5 (1), 1–8.

Bhunya, P.K., Singh, P.K., Mishra, S.K., 2009. Fréchet and chi-square parametric expressions combined with Horton ratios to derive a synthetic unit hydrograph. Hydrol. Sci. J. 54 (2), 274–286.

Bonnin, G.M., Martin, D., Lin, B., Parzybok, T., Yekta, M., Riley, D., 2006. NOAA Atlas 14 Precipitation-Frequency Atlas of the United States Volume 2 Version 3.0: Delaware, District of Columbia, Illinois, Indiana, Kentucky, Maryland, New Jersey, North Carolina, Ohio, Pennsylvania, South Carolina, Tennessee, Virginia, West Virgini. 2, p. 295.

Botter, G., Rinaldo, A., 2003. Scale effect on geomorphologic and kinematic dispersion. Water Resour. Res. 39 (10), 1–10.

Bras, R.L., Rodriguez-Iturbe, I., 1989. A review of the search for a quantitative link between hydrologic response and fluvial geomorphology. In: New Directions for Surface Water Modeling. (181), pp. 149–163.

Burgan, H.I., Aksoy, H., 2022. Daily flow duration curve model for ungauged intermittent subbasins of gauged rivers. J. Hydrol. 604.

Croley, T.E., 1980. Gamma synthetic hydrographs. J. Hydrol. 47 (1-2), 41-52.

- Davis, C., Brown, B., Bullock, R., 2006. Object-based verification of precipitation forecasts. Part II: Application to convective rain systems. Mon. Weather Rev. 134 (7), 1785–1795.
- de Lima, J.L., Singh, V.P., 2003. Laboratory experiments on the influence of storm movement on overland flow. Phys. Chem. Earth 28 (6–7), 277–282.
- Di Lazzaro, M., Volpi, E., 2011. Effects of hillslope dynamics and network geometry on the scaling properties of the hydrologic response. Adv. Water Resour. 34 (11), 1496–1507
- Dixon, M., Wiener, G., 1993. TITAN: Thunderstorm identification, tracking, analysis, and nowcasting—A radar-based methodology. J. Atmos. Ocean. Technol. 10 (6), 785–797.
- Dooge, J., 1973. Linear Theory of Hydrologic Systems. (1468), Agricultural Research Service, US Department of Agriculture.
- Du, J., 2011. GCIP/EOP Surface: Precipitation NCEP/EMC 4KM Gridded Data (GRIB) Stage IV Data. Version 1.0. UCAR/NCAR - Earth Observing Laboratory.
- Emmanuel, I., Andrieu, H., Leblois, E., Janey, N., Payrastre, O., 2015. Influence of rainfall spatial variability on rainfall-runoff modelling: Benefit of a simulation approach? J. Hydrol, 531, 337–348.
- Foroud, N., Broughton, R.S., Austin, G.L., 1984. The effects of a moving rainstorm on direct runoff properties. J. Am. Water Resour. Assoc. 20 (1), 87–91.
- Gao, S., Fang, Z.N., 2019. Investigating hydrologic responses to spatio-temporal characteristics of storms using a Dynamic Moving Storm generator. Hydrol. Process. 33 (21), 2729–2744.
- Ghimire, G., Jadidoleslam, N., Goska, R., Krajewski, W.F., 2021. Insights into storm direction effect on flood response. J. Hydrol. 600, 126683.
- Ghimire, G.R., Krajewski, W.F., Ayalew, T.B., Goska, R., 2022. Hydrologic investigations of radar-rainfall error propagation to rainfall-runoff model hydrographs. Adv. Water Resour. 161 (January), 104145.
- Goodwell, A.E., 2020. "It's raining bits": Patterns in directional precipitation persistence across the United States. J. Hydrometeorol. 21 (12), 2907–2921.
- Grimaldi, S., Petroselli, A., Alonso, G., Nardi, F., 2010. Flow time estimation with spatially variable hillslope velocity in ungauged basins. Adv. Water Resour. 33 (10), 1216–1223.
- Grimaldi, S., Petroselli, A., Nardi, F., 2012. A parsimonious geomorphological unit hydrograph for rainfall-runoff modelling in small ungauged basins. Hydrol. Sci. J. 57 (1), 73–83.
- Guo, J., 2022. General and analytic unit hydrograph and its applications. J. Hydrol. Eng. 27 (2), 1–8.
- Guo, J., Asce, M., 2022. General unit hydrograph from chow's linear theory of hydrologic systems and its applications. 1, (10), pp. 1–10.
- Gupta, V.K., Waymire, E., Wang, C.T., 1980. A representation of an instantaneous unit hydrograph from geomorphology. Water Resour. Res. 16 (5), 855–862.
- Huang, P.-C., Lee, K.T., 2023. A novel method of estimating dynamic partial contributing area for integrating subsurface flow layer into GIUH model. J. Hydrol. 617, 128981.
- Jadidoleslam, N., Hornbuckle, B.K., Krajewski, W.F., Mantilla, R., Cosh, M.H., 2022. Analyzing effects of crops on SMAP satellite-based soil moisture using a rainfall-runoff model in the U.S. corn belt. IEEE J. Sel. Top. Appl. Earth Obs. Remote Sens. 15, 247–260.
- Kim, J., Lee, J., Kim, D., Kang, B., 2019. The role of rainfall spatial variability in estimating areal reduction factors. J. Hydrol. 568 (June 2018), 416–426.
- Kirkby, M.J., 1976. Tests of the random network model, and its application to basin hydrology. Earth Surf. Process. 1 (3), 197–212.
- Lagarias, J.C., Reeds, J.A., Wright, M.H., Wright, P.E., 1998. Convergence properties of the Nelder-Mead simplex method in low dimensions. SIAM J. Optim. 9 (1), 112-147.
- Li, Z., Wright, D.B., Zhang, S.Q., Kirschbaum, D.B., Hartke, S.H., 2020. Object-based comparison of data-driven and physics-driven satellite estimates of extreme rainfall. J. Hydrometeorol. 21 (12), 2759–2776.
- Mbengue, C., Schneider, T., 2013. Storm track shifts under climate change: What can be learned from large-scale dry dynamics. J. Clim. 26 (24), 9923–9930.
- Merz, B., Basso, S., Fischer, S., Lun, D., Blöschl, G., Merz, R., Guse, B., Viglione, A., Vorogushyn, S., Macdonald, E., Wietzke, L., Schumann, A., 2022. Understanding heavy tails of flood peak distributions. Water Resour. Res. 1–37.
- Mesa, O.J., Mifflin, E.R., 1986. On the relative role of hillslope and network geometry in hydrologic response. In: Gupta, V.K., Rodríguez-Iturbe, I., Wood, E.F. (Eds.), Scale Problems in Hydrology: Runoff Generation and Basin Response. Springer Netherlands, Dordrecht, pp. 1–17.
- Moussa, R., 2008a. Effect of channel network topology, basin segmentation and rainfall spatial distribution on the geomorphologic instantaneous unit hydrograph transfer function. Hydrol. Process. 22 (3), 395–419.
- Moussa, R., 2008b. What controls the width function shape, and can it be used for channel network comparison and regionalization? Water Resour. Res. 44 (8), 1–19.
- Murphey, J.B., Wallace, D.E., Lane, L.J., 1977. Geomorphic parameters predict hydrograph characteristics in the southwest. J. Am. Water Resour. Assoc. 13 (1), 25–37.
- Naden, P., Broadhurst, P., Tauveron, N., Walker, A., 1999. River routing at the continental scale: use of globally-available data and an a priori method of parameter estimation. Hydrol. Earth Syst. Sci. 3 (1), 109–123.

- Ngirane-Katashaya, G.G., Wheater, H.S., 1985. Hydrograph sensitivity to storm kinematics. Water Resour. Res. 21 (3), 337-345.
- Patel, J.N., Thorvat, A.R., 2016. Synthetic unit hydrograph development for ungauged basins using dimensional analysis. J. Am. Water Works Assoc. 108 (3), E145–E153.
- Perez, G., Gomez-Velez, J.D., Mantilla, R., Wright, D.B., Li, Z., 2021. The effect of storm direction on flood frequency analysis. Geophys. Res. Lett. 48 (9), 1–10.
- Perez, G., Mantilla, R., Krajewski, W.F., 2018. The influence of spatial variability of width functions on regional peak flow regressions. Water Resour. Res. 54 (10), 7651–7669.
- Perez, G., Mantilla, R., Krajewski, W.F., Quintero, F., 2019a. Examining observed rainfall, soil moisture, and river network variabilities on peak flow scaling of rainfall-runoff events with implications on regionalization of peak flow quantiles. Water Resour. Res. 55 (12), 10707–10726.
- Perez, G., Mantilla, R., Krajewski, W.F., Wright, D.B., 2019b. Using physically based synthetic peak flows to assess local and regional flood frequency analysis methods. Water Resour. Res. 55 (11), 8384–8403.
- Prein, A.F., Liu, C., Ikeda, K., Bullock, R., Rasmussen, R.M., Holland, G.J., Clark, M., 2020. Simulating North American mesoscale convective systems with a convection permitting climate model. Clim. Dynam..
- Quintero, F., Krajewski, W.F., Seo, B.-C., Mantilla, R., 2019. Improvement and evaluation of the iowa flood center hillslope link model (HLM) by calibration-free approach. J. Hydrol. 584 (November 2019), 124686.
- Rigon, R., Bancheri, M., Formetta, G., de Lavenne, A., 2016. The geomorphological unit hydrograph from a historical-critical perspective. Earth Surf. Process. Landforms 41 (1), 27–37.
- Rinaldo, A., Marani, A., Rigon, R., 1991. Geomorphological dispersion. Water Resour. Res. 27 (4), 513–525.
- Rinaldo, A., Rodruiguez-Iturbe, I., 1996. Geomorphological theory of the hydrological response. Hydrol. Process. 10 (6), 803–829.
- Rinaldo, A., Vogel, G.K., Rigon, R., Rodriguez-Iturbe, I., 1995. Can one gauge the shape of a basin? Water Resour. Res. 31 (4), 1119–1127.
- Rodríguez-Iturbe, I., Valdés, J.B., 1979. The geomorphologic structure of hydrologic response. Water Resour. Res. 15 (6), 1409–1420.
- Seo, Y., Schmidt, A.R., 2013. Network configuration and hydrograph sensitivity to storm kinematics. Water Resour. Res. 49 (4), 1812–1827.
- Seo, Y., Schmidt, A.R., Sivapalan, M., 2012. Effect of storm movement on flood peaks: Analysis framework based on characteristic timescales. Water Resour. Res. 48 (5), 1–12.
- Sherman, L.K., 1932. Stream flow from rainfall by the unit graph method. Eng. News Rec. (108), 501–505.
- Singh, K.P., 1964. Nonlinear instantaneous unit-hydrograph theory. J. Hydraul. Div. 90 (2), 313–347.
- Singh, V.P., 1997. Effect of spatial and temporal variability in rainfall and watershed characteristics on stream flow hydrograph. Hydrol. Process. 11 (12), 1649–1669.
- Singh, V.P., 2002. Effect of the duration and direction of storm movement on planar flow with full and partial areal coverage. Hydrol. Process. 16 (17), 3437–3466.
- Singh, P., Mishra, S., Jain, M., 2014. A review of the synthetic unit hydrograph: from the empirical UH to advanced geomorphological methods. Hydrol. Sci. J. 59 (2), 239–261.
- Smart, J.S., Surkan, A.J., 1967. The relation between mainstream length and area in drainage basins. Water Resour. Res. 3 (4), 963–974.
- Smith, J.A., Baeck, M.L., Meierdiercks, K.L., Nelson, P.A., Miller, A.J., Holland, E.J., 2005. Field studies of the storm event hydrologic response in an urbanizing watershed. Water Resour. Res. 41 (10).
- Smith, J.a., Baeck, M.L., Villarini, G., Wright, D.B., Krajewski, W., 2013. Extreme flood response: The june 2008 flooding in iowa. J. Hydrometeorol. 14 (6), 1810–1825.
- Snell, J.D., Sivapalan, M., 1994. On geomorphological dispersion in natural catchments and the geomorphological unit hydrograph. Water Resour. Res. 30 (7), 2311–2323.Snyder, F.F., 1938. Synthetic unit-graphs. Trans. Am. Geophys. Union 19 (1), 447.
- Tamarin-Brodsky, T., Kaspi, Y., 2017. Enhanced poleward propagation of storms under climate change. Nat. Geosci. 10 (12), 908–913.
- Taylor, A.B., Schwarz, H.E., 1952. Unit-hydrograph lag and peak flow related to basin characteristics. Trans. Am. Geophys. Union 33 (2), 235.
- van de Nes, T., 1973. Linear analysis of a physically based model of a distributed surface runoff system.
- Velasquez, N., Mantilla, R., Krajewski, W.F., Quintero, F., Zanchetta, A., 2022. Identification and regionalization of streamflow routing parameters for the HLM hydrological model in Iowa. Jamess.
- Volpi, E., Di Lazzaro, M., Fiori, A., 2013. Analytical modeling of the hydrologic response under moving rainstorms: Storm–catchment interaction and resonance. J. Hydrol. 493, 132–139.
- Watts, L., Calver, A., 1991. Effects of spatially-distributed rainfall on runoff for a conceptual catchment. Hydrol. Res. 22 (1), 1–14.
- Wright, D.B., Mantilla, R., Peters-Lidard, C.D., 2017. A remote sensing-based tool for assessing rainfall-driven hazards. Environ. Model. Softw. 90, 34–54.
- Wright, D.B., Smith, J.A., Baeck, M.L., 2014. Critical examination of area reduction factors. J. Hydrol. Eng. 19 (4), 769–776.
- Yen, B.C., Lee, K.T., 1997. Unit hydrograph derivation for ungauged watersheds by stream-order laws. J. Hydrol. Eng. 2 (1), 1–9.

- Yi, B., Chen, L., Zhang, H., Singh, V.P., Jiang, P., Liu, Y., Guo, H., Qiu, H., 2022. A time-varying distributed unit hydrograph method considering soil moisture. Hydrol. Earth Syst. Sci. 26 (20), 5269–5289.
- Yu, G., Wright, D.B., Li, Z., 2020. The upper tail of precipitation in convection-permitting regional climate models and their utility in nonstationary rainfall and flood frequency analysis. Earth's Future 8 (August), 1–18.
- Yu, G., Wright, D.B., Zhu, Z., Smith, C., Holman, K.D., 2019. Process-based flood frequency analysis in an agricultural watershed exhibiting nonstationary flood seasonality. Hydrol. Earth Syst. Sci. 23 (5), 2225–2243.
- Zhu, Z., Wright, D.B., Yu, G., 2018. The impact of rainfall space-time structure in flood frequency analysis. Water Resour. Res. 54 (11), 8983–8998.